Article

Carbohydrate-Based DNA Ligands: Sugar–Oligoamides as a Tool to Study Carbohydrate–Nucleic Acid Interactions

Jason N. Martin, Eva M. Muoz, Caroline Schwergold, Florence Souard, Juan Luis Asensio, Jess Jimnez-Barbero, Javier Caada, and Cristina Vicent

J. Am. Chem. Soc., **2005**, 127 (26), 9518-9533• DOI: 10.1021/ja050794n • Publication Date (Web): 08 June 2005

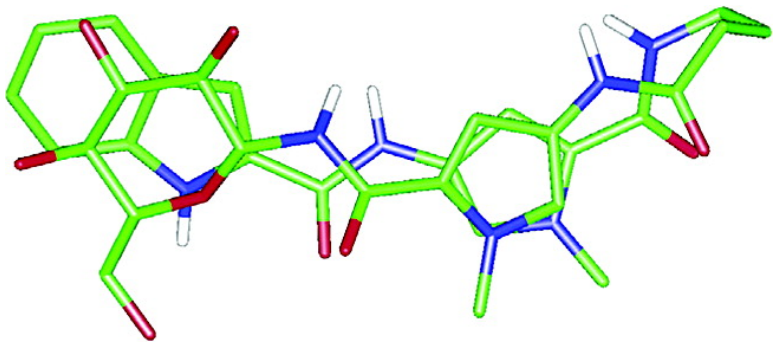

J|A|C|S
ARTICLES
Published on Web 06/08/2005

Carbohydrate-Based DNA Ligands: Sugar−Oligoamides as a Tool to Study Carbohydrate−Nucleic Acid Interactions

Jason N. Martin,[†] Eva M. Muñoz,[†] Caroline Schwergold,[†] Florence Souard,[†] Juan Luis Asensio,[†] Jesús Jiménez-Barbero,[‡] Javier Cañada,[‡] and Cristina Vicent*[,†]

Contribution from the Instituto de Química Orgánica, CSIC, c/ Juan de la Cierva 3, Madrid 28006, Spain, and Centro de Investigaciones Biológicas, CSIC, c/ Ramiro de Maeztu 9, Madrid 28040, Spain

Received February 7, 2005; E-mail: iqocv18@iqog.csic.es

Abstract: Sugar−oligoamides have been designed and synthesized as structurally simple carbohydrate-based ligands to study carbohydrate−DNA interactions. The general design of the ligands **1**−**3** has been done as to favor the bound conformation of Distamycin-type γ-linked covalent dimers which is a hairpin conformation. Indeed, NMR analysis of the sugar−oligoamides in the free state has indicated the presence of a percentage of a hairpin conformation in aqueous solution. The DNA binding activity of compounds **1**−**3** was confirmed by calf thymus DNA (*ct*-DNA) NMR titration. Interestingly, the binding of the different sugar−oligoamides seems to be modulated by the sugar configuration. Semiquantitative structural information about the DNA ligand complexes has been derived from NMR data. A *competition experiment* with Netropsin suggested that the sugar−oligoamide **3** bind to DNA in the minor groove. The NMR titrations of **1**-**3** with poly(dA-dT) and poly(dG-dC) suggested *preferential binding* to the ATAT sequence. TR-NOE NMR experiments for the sugar−oligoamide **3**−*ct*-DNA complex both in D_2O and H_2O have confirmed the complex formation and given information on the *conformation of the ligand in the bound state.* The data confirmed that the sugar−oligoamide ligand is a hairpin in the bound state. Even more relevant to our goal, structural information on the conformation around the *N*-glycosidic linkage has been accessed. Thus, *the sugar asymmetric centers* pointing to the NH-amide and *N*-methyl rims of the molecule have been characterized.

Introduction

Carbohydrates are present in many antibiotics and anticancer drugs that bind DNA.[1,2] Carbohydrate minor groove DNA binders are neutral neoglycoconjugates whose sugar residues are deoxygenated, thus showing a delicate balance between hydrophilic and hydrophobic domains.[3] The three-dimensional structure of these oligosaccharides is linear and slightly curved to fit the minor groove of DNA.[4] Traditionally, the glycan chains of these DNA glycoconjugate binders have been viewed as molecular elements that control the pharmacokinetics of a drug, such as absorption, distribution, metabolism, and excretion. This notion changed a few years ago with the finding that the carbohydrate residues present in the Calicheamicin antibiotics partially determine the selectivity of the process.[5−9] The role of the carbohydrate became even more relevant with the finding that Calicheamicin methyl glycoside inhibits the formation of DNA−protein complexes at micromolar concentrations in a sequence specific manner.[10]

However, the lack of knowledge on basic aspects of the interactions at the origin of selectivity and specificity of carbohydrate−nucleic acid binding makes it difficult to effectively design new carbohydrate−nucleic acid binders.[11−15]

We have previously explored the use of carbohydrate hydrogen bonding cooperativity[16−18] as a tool to bind carbohydrates to the H-bonding motifs present in the grooves of DNA.

[†] Instituto de Química Orgánica.
[‡] Centro de Investigaciones Biológicas.

(1) Krugh, T. R. *Curr. Opin. Struct. Biol.* **1994**, *4*, 351−364.
(2) Kahne, D. *Chem. Biol.* **1995**, *2*, 7−12.
(3) Kirschning, A.; Bechthold, A. F.-W.; Rohr, J. *Top. Curr. Chem.* **1997**, *184*, 1−84.
(4) Walker, S.; Valentine, K. G.; Kahne, D. *J. Am. Chem. Soc.* **1990**, *112*, 6428−6429.
(5) Drak, J.; Iwasawa, N.; Danishefsky, S.; Crothers, D. M. *Proc. Natl. Acad. Sci. U.S.A.* **1991**, *88*, 7464−7468.
(6) Zein, N.; Poncin, M.; Nilakantan, R.; Ellestad, G. A. *Science* **1989**, *244*, 697−699.
(7) Danishefsky, S. J.; Shair, M. D. *J. Org. Chem.* **1996**, *61*, 16−44.
(8) Walker, S.; Murnick, J.; Kahne, D. *J. Am. Chem. Soc.* **1993**, *115*, 7954−7961.
(9) Biswas, K.; Pal, S.; Carbeck, J. D.; Kahne, D. *J. Am. Chem. Soc.* **2000**, *122*, 8413−8420.
(10) Moreover, it rapidly dissociates preformed complexes not only in vitro but also in vivo, blocking the expression of a reporter gene under the control of the transcription factor NFAT. (a) Nicolau, K. C.; Tsay, S.-C.; Suzuki, T.; Joyce, G. F. *J. Am. Chem. Soc.* **1992**, *114*, 7555−7557. (b) Bifulco, G.; Galeone, A.; Gomez-Paloma, L.; Nicolau, K. C.; Chazin, W. J. *J. Am. Chem. Soc.* **1996**, *118*, 8817−8824. (c) Ho, S. N.; Boyer, S. H.; Schreilser, S. L.; Danishefsky, S. J.; Crabtree, G. R. *Proc. Natl. Acad. Sci. U.S.A.* **1994**, *91*, 9203−9207. (d) Sissi, C.; Aiyar, J.; Boyer, S.; Depew, K.; Danishfsky, S.; Crothers, D. M. *Proc. Natl. Acad. Sci. U.S.A.* **1999**, *96*, 10643−10648.
(11) Sakurai, K.; Shinkai, S. *J. Am. Chem. Soc.* **2000**, *122*, 4520−4521.
(12) Ding, W.-d.; Ellestad, G. A. *J. Am. Chem. Soc.* **1991**, *113*, 6617−6620.
(13) Depew, K. M.; Zeman, S. M.; Boyer, S. H.; Denhart, D. J.; Ikemoto, N.; Danishefsky, S. J.; Crothers, D. M. *Angew. Chem., Int. Ed. Engl.* **1996**, *35*, 2797−2801.
(14) Xuereb, H.; Maletic, M.; Gildersleeve, J.; Pelczer, I.; Kahne, D. *J. Am. Chem. Soc* **2000**, *122*, 1883−1890.
(15) Wu, M.; Stoermer, D.; Tullius, T. D.; Townsend, C. A. *J. Am. Chem. Soc* **2000**, *122*, 12884−12885.

10.1021/ja050794n CCC: $30.25

Scheme 1. Hairpin/Linear Conformers in Equilibrium

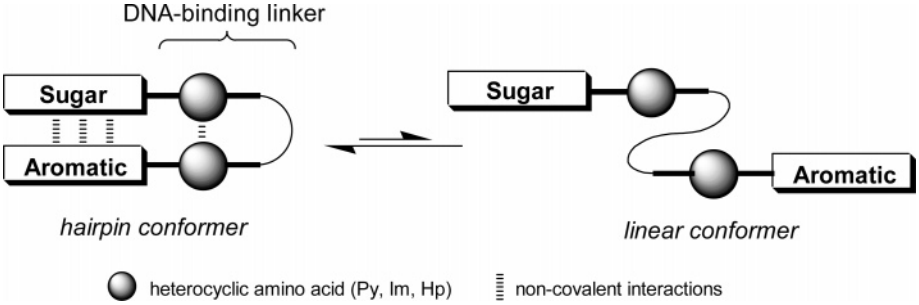

Thus, we have characterized the sugar H-bonding patterns that efficiently bind CG[19] base pairs and phosphate[20] in non polar solvents. In this paper, we present a strategy that extends our work to natural systems, with the aim of obtaining information about the structural requirements for DNA groove recognition by sugars in aqueous media. With this purpose in mind, a series of sugar−oligoamides have been designed and synthesized as a tool to study carbohydrate−DNA structural requirements (Scheme 1). The oligoamide fragment, selected as DNA linker, resembles those of the naturally occurring antibiotics such as Distamycin A and Netropsin. These oligoamides are known to bind DNA in the minor groove as antiparallel dimers.[21,22] Moreover, it has been shown that covalently linking such dimers dramatically increases the DNA binding affinity through the opportunity for face-to-face pairing of the heterocyclic rings. These investigations have culminated in the development of ring-pairing rules by which oligoamides can be constructed from *N*-methylpyrrole, -imidazole, and -hydroxypyrrole amino acids with predictable DNA sequence selective binding.[23−26] Recently, these oligoamides have been probed to inhibit transcription in vivo.[27−29] The design of our carbohydrate-containing DNA ligands is based on these previous data. Thus, we have selected the side-by-side pairing of pyrrole amino acids (Py) covalently joined head-to-tail by a γ-amino butyric acid linker (γ). We expected the Py/Py pair[30] to be the minimum oligoamide structure able to retain DNA binding ability, thus allowing DNA−carbohydrate proximity. Additionally, the γ linker is known to be the most suitable alkyl chain length for hairpin formation.[31] We have included an indole ring[32] at the N-terminus in order to drive the linear/hairpin equilibrium (Scheme 1) toward the folded conformation through carbohydrate/aromatic CH−π interactions[33,34] which is the conformation which interacts with DNA. In addition, the indole-2-carboxamide was selected as an extended mimic of the pyrrole amino acid, which maintains the necessary crescent geometry of the oligoamide. Clearly, the configuration and conformation of the bond that links the sugar to the oligoamide will be a decisive factor in determining the position of the equilibrium. We decided to prepare the C-1 amido-sugars which, taking into account the predicted conformation for anomeric amides,[35,36] could generate the hairpin conformer. The C-1 linkage, in principle, would make possible generating a preferred orientation of the sugar within the hairpin structure and, hence, "conformational restriction". The different relative configuration of the asymmetric centers in the sugar can also play a role in defining the face selection, and thus, a particular orientation of the sugar will be exposed toward the floor of the minor groove. This feature will be relevant in the further design of sugars with particular hydrophilic or hydrophobic residues oriented toward the minor groove.

Thus, starting from the conformation corresponding to Dervan's oligoamides bound to DNA in solution,[37] molecular models of the sugar−oligoamides with the oligoamide in C-1 were built and minimized. Careful inspection of the models obtained with the anomeric linkage α and β strongly suggests that a β-linkage in the sugar moiety is required in order to allow a proper pyranose−indole stacking (see Figure 1).

As a first step, sugar−oligoamides from galactose β-Gal-Py-γ-Py-Ind **1**, glucose β-Glc-Py-γ-Py-Ind **2**, and xylose β-Xyl-Py-γ-Py-Ind **3**, were prepared (see Figure 2). The conformation of **1**−**3** in the free state was analyzed by NMR methods. Then, the DNA binding activity of the sugar−oligoamides has been tested. Thus, NMR titration experiments with *ct*-DNA, poly (dA-dT), and poly (dG-dC) conclusively show that all synthesized ligands bind to DNA. Moreover, a qualitative description of the mode of interaction has been accomplished through the use TR-NOESY NMR experiments.

(16) Lopez de la Paz, M.; Ellis, G.; Penadés, S.; Vicent, C. *Tetrahedron Lett.* **1997**, *38*, 1659−1662.
(17) Lopez de la Paz, M.; Jiménez-Barbero, J.; Vicent, C. *Chem. Commun.* **1998**, 465−466.
(18) Luque, F. J.; López, J. M.; López de la Paz, M.; Vicent, C.; Orozco, M. *J. Phys. Chem. A* **1998**, *102*, 6690−6696.
(19) López de la Paz, M.; González, C.; Vicent, C. *Chem. Commun.* **2000**, 411−412.
(20) Muñoz, E. M.; López de la Paz, M.; Jiménez-Barbero, J.; Ellis, G.; Pérez, M.; Vicent, C. *Chem.—Eur. J.* **2002**, *8*, 1908−1914.
(21) Pelton, J. G.; Wemmer, D. E. *Proc. Natl. Acad. Sci. U.S.A.* **1989**, *86*, 5723−5727.
(22) Pelton, J. G.; Wemmer, D. E. *J. Am. Chem. Soc.* **1990**, *112*, 1393−1399.
(23) Dervan, P. B.; Bürli, R. W. *Curr. Opin. Chem. Biol.* **1999**, *3*, 688−693.
(24) White, S.; Szewczyk, J. W.; Turner, J. M.; Baird, E. E.; Dervan, P. B. *Nature* **1998**, *392*, 468−471.
(25) Geierstanger, B. H.; Mrksich, M.; Dervan, P. B.; Wemmer, D. E. *Science* **1994**, *266*, 646−650.
(26) Wemmer, D. E.; Dervan, P. B. *Curr. Opin. Struct. Biol.* **1997**, *7*, 355−361.
(27) Janssen, S.; Durussel, T.; Laemmli, U. K. *Mol. Cell* **2000**, *6*, 999−1011.
(28) Janssen, S.; Cuvier, O.; Müller, M.; Laemmli, U. K. *Mol. Cell* **2000**, *6*, 1013−1024.
(29) Henikoff, S.; Vermaak, D. *Cell* **2000**, *103*, 695−698.
(30) Dervan, P. B. *Science* **1986**, *232*, 464−471.
(31) Mrksich, M.; Parks, M. E.; Dervan, P. B. *J. Am. Chem. Soc.* **1994**, *116*, 7983−7988.
(32) Schnell, J. R.; Ketchem, R. R.; Boger, D. L.; Chazin, W. J. *J. Am. Chem. Soc.* **1999**, *121*, 5645−5652.
(33) The indole sidechain of the tryptophan amino acid is present in many lectin binding sites and is known to contribute to sugar binding through CH− interactions. (a) Asensio, J. L.; Cañada, F. J.; Siebert, H.-C.; Laynez, J.; Poveda, A.; Nieto, P. N.; Soedjanaamadja, U. M.; Gabius, H.-J.; Jimenéz-Barbero, *J. Chem. Biol.* **2000**, *7*, 529−543. (b) Jimenéz-Barbero, J.; Asensio, J. L.; Cañada, F. J.; Poveda, A. *Curr. Opin. Struct. Biol.* **1999**, *9*, 549−555.
(34) Muraki, M. *Protein Pept. Lett.* **2002**, *9*, 195−209.
(35) Avalos, M.; Babiano, R.; Carretero, M. J.; Cintas, P.; Higes, F. J.; Jiménez, J. L.; Palacios, J. C. *Tetrahedron* **1998**, *54*, 615−628.
(36) Masuda, M.; Shimizu, T. *Carbohydr. Res.* **2000**, *326*, 56−66.
(37) Hawkins, C. A.; Peláez de Clairac, R.; Dominey, R. N.; Baird, E. E.; White, S.; Dervan, P. B.; Wemmer, D. E. *J. Am. Chem. Soc.* **2000**, *122*, 5235−5243.

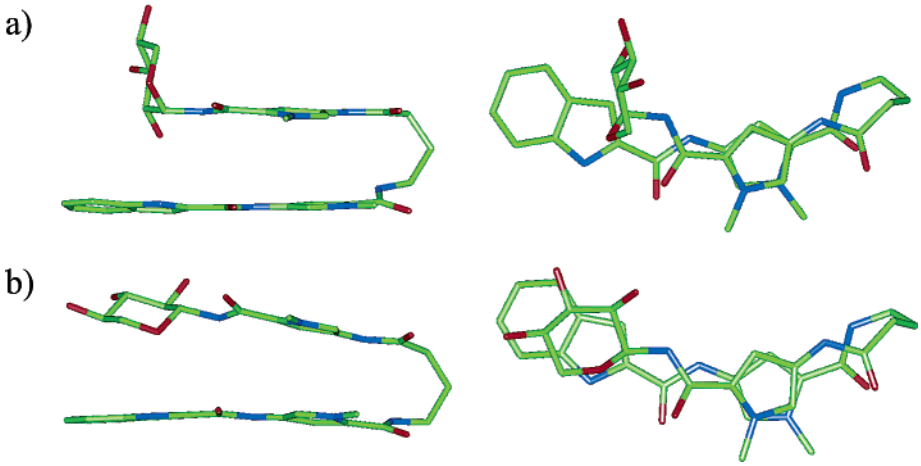

Figure 1. Molecular model of α-Xyl-Py-γ-Py-Ind (a) and β-Xyl-Py-γ-Py-Ind **3** (b). Both views (left and right) are related by a 90° rotation around the *x*-axis.

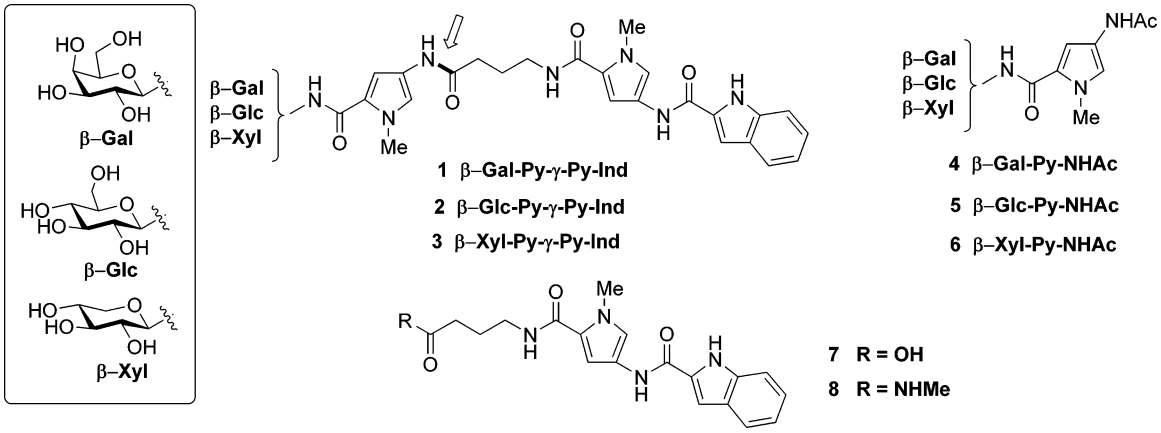

Figure 2. Sugar−oligoamides and oligamides' models.

Results and Discussion

Accordingly, we have prepared the sugar−oligoamides β-Gal-Py-γ-Py-Ind **1**, β-Glc-Py-γ-Py-Ind **2**, and β-Xyl-Py-γ-Py-Ind **3** (Figure 2) by a convergent route. Thus, the chains are built up from two separate suitably protected strands, forming the final amide linkage (arrowed) at a late stage. These sugar oligoamides were selected to determine the influence of the sugar stereochemistry on the preferred conformation of these glycoconjugates in the free state and once bound to DNA through subtle differences in the sugar moieties/configuration. The galactose β-Gal-Py-γ-Py-Ind **1** presents an axially oriented OH at position 4 of the sugar β face, while glucose derivative **2** places a hydrogen atom at this position. Xylose oligoamide **3** is a glucose analogue that lacks the 6-hydroxymethyl group, thus increasing the number of C−H in the β face.

Additionally, the corresponding sugar strand amides β-Gal-Py-NHAc **4**, β-Glc-Py-NHAc **5**, and β-Xyl-Py-NHAc **6**, the indole strand acid HO-γ-Py-Ind **7**, and the analogous amide MeNH-γ-Py-Ind **8** were prepared for comparative purposes (Figure 2). Those fragments common to all of the sugar oligoamides **1**−**3** were prepared as models of the unfolded conformation. Thus, conformational analysis of compounds **1**−**8** was carried out in D_2O/[D_6]-acetone (9:1), D_2O/H_2O mixtures (phosphate buffer).

Synthesis. Our convergent synthesis started with the preparation of the sugar strand fragments **9**, **10**, and **11** (Scheme 2). Thus, commercial galactose pentaacetate was converted to the C-1 azide[38,39] and reduced (H_2, Pd) to the corresponding amine **12**[40] (96%, two steps). 1-Methyl-4-nitropyrrole-2-carboxylic acid **13**[41] was prepared for coupling with protected amine **12** by activation of the acid with DIPC and HOBt or by conversion to the acid chloride **14**[42,43] to afford the target nitropyrrole amide **9** (86% and 87%, respectively). Similarly, the β-galactosylamine **15**[42,43] and the β-xylosylamine **16** were converted to the amides **10** and **11**, respectively. The nitro function represents a latent amino group (revealed by hydrogenation), so avoiding excessive manipulation of the unstable aminopyrroles. Nitropyrrole **9** (an intermediate of the target sugar oligoamide **3**) also serves as a precursor of the galactose strand model compound **4** through hydrogenation and *N*-acetylation (nitro- to acetamido-) to give **17**, before acetate cleavage to afford model **4**. Similarly, glucosyl- and xylosyl-pyrroles **10** and **11** were converted to the corresponding sugar strand models **5** and **6** via acetamides **18** and **19**.

Synthesis of the indole strand acid **7** started with ester **20**, prepared from commercial materials, by the haloform methodology of Xiao and co-workers[44] (Scheme 3). Hydrogenation of

(38) Paulsen, H.; Györgydeák, Z.; Friedman, M. *Chem. Ber.* **1974**, *107*, 1568−1578.
(39) Tropper, F. D.; Andersson, F. O.; Braun, S.; Roy, R. *Synthesis* **1992**, 618−620.
(40) Sabesan, S. *Tetrahedron Lett.* **1997**, *38*, 3127−3130.
(41) Baird, E. E.; Dervan, P. B. *J. Am. Chem. Soc.* **1996**, *118*, 6141−6146.
(42) Lown, J. W.; Krowicki, K. *J. Org. Chem.* **1985**, *50*, 3774−3779.
(43) Mrksich, M.; Dervan, P. B. *J. Am. Chem. Soc.* **1993**, *115*, 9892−9899.

Scheme 2 [a]

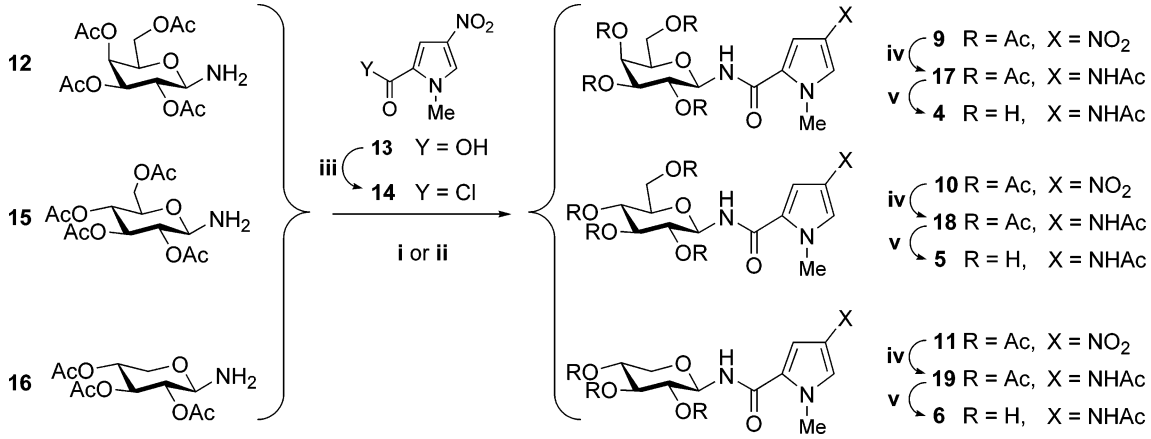

[a] (i) DIPC, HOBt, **13**; (ii) **14**, $CHCl_3$, Et_3N, Δ; (iii) $SOCl_2$, Δ, 1 h; (iv) H_2, Pd−C, MeOH or DCM, then AcCl or Ac_2O, Et_3N, Δ; (v) NaOMe, MeOH, rt, 1 min, then Amberlite IR-120 (H^+) to pH = 6.

Scheme 3 [a]

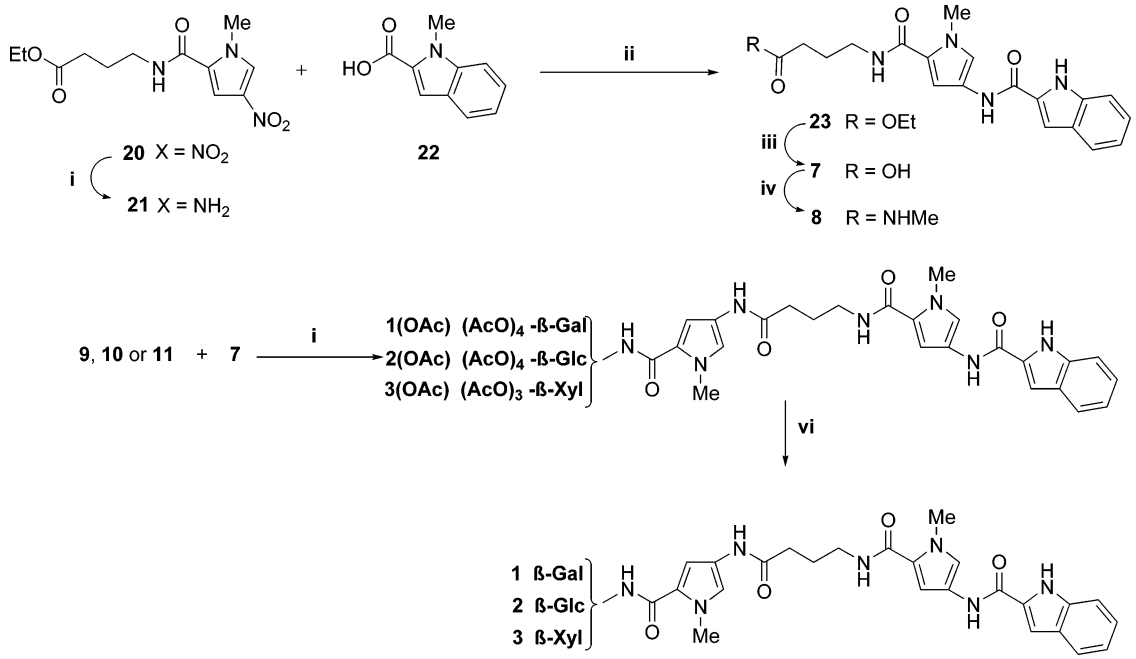

[a] (i) H_2, 10%, Pd−C; (ii) DIPC, HOBt, DCM or DMF; (iii) aq NaOH (1 M), MeOH, 1 min then aq HCl (to pH = 2); (iv) DIPC, HOBt, $H_2NMe{\cdot}HCl$, Et_3N; (vi) NaOMe, MeOH, 1 min then Amberlite IR-120 (H^+) to pH = 6.

20 gave aminopyrrole **21**, used immediately in a carbodiimide-mediated coupling with indole-2-carboxylic acid **22** to afford the ester oligoamide **23**. Chromatography did not remove all traces of the rest of coupling byproduct (diisopropyl urea: DIPU), but hydrolysis of the crude ester **23** (aq NaOH, 1 min) afforded the acid **7**, isolated in pure form. With the required fragments now in hand, the sugar nitropyrroles **9**, **10**, or **11** were separately reduced and the crude amines added to the preformed activated ester of the acid **7** to form the desired protected oligoamides [$(AcO)_4$-*β*-Gal-Py-*γ*-Py-Ind **1(OAc)**, $(AcO)_4$-*β*-Glc-Py-*γ*-Py-Ind **2(OAc)**, and $(AcO)_4$-*β*-Xyl-Py-*γ*-Py-Ind **3(OAc)**]. Instantaneous acetate cleavage with sodium methoxide afforded the target *β*-glycosyl-oligoamides **1**, **2**, and **3**, respectively. The indole strand acid **7** was also used to prepare our final model compound **8** by amide coupling with methylamine.

Structural Characterization and Conformational Studies of 1−8 in Aqueous Solution. It is well-known that the 3D structure and dynamic behavior of a ligand in the free state play an important role in the recognition event. Thus, it has been suggested that, in those cases where the ligand is flexible in solution, the loss of conformational freedom associated to binding constitutes one of the main contributions to the entropic barrier of the process.[45] In this sense, a possible strategy in the design of higher affinity ligands would be to chemically block the ligand in its bioactive conformation.

Recent studies by Wemmer et al. have proved that DNA ligands such as Im-Py-Py-*γ*-Py-Py-Py-*β*-Dp adopt a hairpin geometry in the bound state.[37,46,47] This hairpin structure was defined by NOEs between H-3 protons of the rings stacked

(44) Xiao, J.; Yuan, G.; Huang, W.; Chan, A. S. C.; Lee, K.-L. D. *J. Org. Chem.* **2000**, *65*, 5506−5513.

(45) Williams, D. H.; Stephens, E.; O'Brien, D. P.; Zhou, M. *Angew. Chem., Int. Ed.* **2004**, *43*, 6596−6616.

(46) Pilch, D. S.; Poklar, N.; Gelfand, C. A.; Law, S. M.; Breslauer, K. J.; Baird, E. E.; Dervan, P. B. *Proc. Natl. Acad. Sci. U.S.A.* **1996**, *93*, 8306−8311.

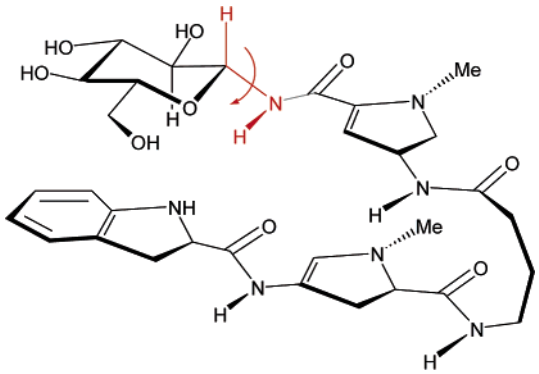

Figure 3. Conformation of the *N*-glycosidic linkage: face selection.

across the groove, as well as analogous contacts between H-5s and the *N*-methyls. Thus, a crescent structure in which the methyls of Py and Im are in one rim (*N*-methyl rim) pointing outside the groove and the NH amides and H-3 of Py and Im are in the opposite rim (*NH*-amide rim) pointing toward the floor of the groove has been described. Interestingly, the free state conformation of these molecules has never been studied in solution. In this context, our sugar−oligoamide derivatives have been carefully designed to fold in a hairpin structure additionally stabilized by sugar−indole CH−π interactions.

To verify the presence of the bioactive (putative bound state) hairpin structure for the sugar−oligoamides in the free state, a conformational study of **1**−**3** has been carried out by NMR, in conjunction with molecular mechanics calculations.

In addition, we can envisage several different conformations depending on the relative orientation of the β-sugar moiety and the indole ring (Figure 3).

Presumably, the most populated structure in solution will be dependent on the sugar stereochemistry. The structural analysis of compounds **1**−**3** solution was carried out by NMR methods. As a first step, a full assignment of the ^{1}H NMR spectra of **1**−**8** in D_2O/[D_6]-acetone (9:1), D_2O and H_2O was obtained using two-dimensional experiments (HMQC, TOCSY, and NOESY).

^{1}H NMR resonances spectra in D_2O/[D_6]-acetone and H_2O/[D_6]-acetone (phosphate buffer, 10 mM, pH = 7) for NH assignment were registered for a total assignment of compounds **1**−**8** (see Tables A−D in the Supporting Information). The first evidence of the existence of a percentage of a particular hairpin conformation in the free state was obtained by comparison of the chemical shifts of the sugar−oligoamides **1**−**3** with those of the indole strand amide **8** (which is common to the three sugar−oligoamides) and the sugar strand models **4**−**6**. It is well-known that the proximity of aromatic rings induces chemical shift changes in the ^{1}H NMR spectrum. Tables 1−4 show the $\Delta\delta_H$ of the proton resonances of each of the sugar oligoamides **1**−**3** and the corresponding sugar strand amides **4**−**6** and the indole strand acid **7** (the indole strand amide **8** was not used due to the low solubility of the product). The chemically induced shifts (CISs) for all the resonances follow the same trend in both D_2O [D_6]-acetone (Table 1) and D_2O solution (Table 2), but the relative differences are much larger in water. Proton resonances of the Py rings (P^{3A}, P^{3B}, P^{5A}, and P^{5B}) were shielded in comparison with their correspondent single strand models and showed the largest shifts within all the proton resonances. The same behavior was found for the methyl N−Py resonances.

The sign of the chemically induced shift (CIS) of the Py signals (P^3, P^5, and CH_3) is compatible with the presence of some extent of an intramolecular folded conformation in which the aromatic residues of each strand are stacked. The comparison of $\Delta\delta$ of the three sugar−oligoamides did not show significant differences depending on the sugar stereochemistry derivative at the C-terminus (Table 2).

Of even greater relevance to the design were the CISs of the sugar ring resonances when the sugar−oligoamides (**1**−**3**) and the correspondent sugar strand derivatives (**4**−**6**) were compared (Table 3) in D_2O.

Table 1. ^{1}H NMR Chemically Induced Shift (CIS) Differences between Sugar−Oligoamides Resonance of **1**−**3** and Their Corresponding Sugar Strand **4**−**6** and Indol Strand **7** in D_2O/Acetone [9:1]

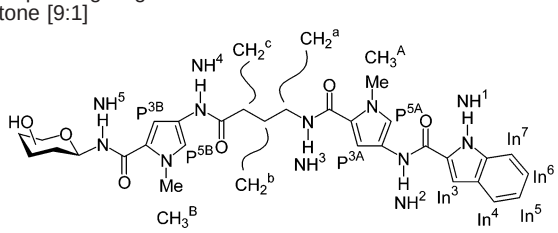

	Gal $\Delta\delta_H$ [**1**–**4**] $\Delta\delta_H$ [(**1**–**7**)]	Glc $\Delta\delta_H$ [**2**–**5**] $\Delta\delta_H$ [(**2**–**7**)]	Xyl $\Delta\delta_H$ [**3**–**6**] $\Delta\delta_H$ [(**3**–**7**)]
In^3	(+0.031)	(−0.032)	(−0.036)
In^4	(−0.047)	(−0.052)	(+0.008)
In^5	(−0.044)	(−0.041)	(+0.009)
In^6	(−0.043)	(−0.042)	(+0.006)
In^7	(−0.002)	(−0.027)	(+0.009)
P^{3A}	(+0.028)	(−0.043)	(−0.145)
P^{5A}	(−0.002)	(−0.093)	(−0.150)
P^{3B}	+0.089	−0.041	−0.113
P^{5B}	+0.063	−0.071	−0.197
CH_3^A	(0)	(−0.072)	(−0.101)
CH_3^B	+0.014	−0.091	−0.147
CH_2^a	(+0.082)	(+0.060)	?
CH_2^b	(+0.136)	(+0.124)	(+0.166)
CH_2^c	(+0.217)	(+0.187)	(+0.190)
sugar	0.048−0.025	−0.019	−0.137
		−0.051	−0.150
H_1	+0.019	−0.050	−0.158

Table 2. ^{1}H NMR Chemically Induced Shift (CIS) Differences between Sugar−Oligoamide Resonances, Excluding the Carbohydrate Protons of **1**−**3** and Their Corresponding Sugar Strands **4**−**6** and Indol Strand **7** in D_2O (Phosphate Buffer)

	Gal $\Delta\delta_H$ [**1**–**4**] $\Delta\delta_H$ [(**1**–**7**)]	Glc $\Delta\delta_H$ [**2**–**5**] $\Delta\delta_H$ [(**2**–**7**)]	Xyl $\Delta\delta_H$ [**3**–**6**] $\Delta\delta_H$ [(**3**–**7**)]
In^3	(−0.059)	(−0.047)	(−0.049)
In^4	(0)	(+0.004)	(+0.008)
In^5	(0)	(+0.008)	(+0.011)
In^6	(−0.006)	(+0.001)	(+0.004)
In^7	(+0.001)	(+0.006)	(+0.009)
P^{3A}	(−0.270)	(−0.238)	(−0.217)
P^{5A}	(−0.142)	(−0.157)	(−0.170)
P^{3B}	−0.149	−0.164	−0.166
P^{5B}	−0.262	−0.264	−0.285
CH_3^A	(−0.092)	(−0.100)	(−0.110)
CH_3^B	−0.214	−0.214	−0.199
CH_2^a	?	?	(+0.099)
CH_2^b	(+0.194)	(+0.183)	(+0.193)
CH_2^c	(+0.167)	(+0.170)	(+0.170)

(47) Pelaez Lamanie de Clairac, R. P. L.; Geierstanger, B. H.; Mrksich, M.; Dervan, P. B.; Wemmer, D. E. *J. Am. Chem. Soc.* **1997**, *119*, 7909−7916.

Table 3. ^{1}H NMR Chemically Induced Shift (CIS) Differences between Carbohydrate Residue of Sugar−Oligoamides **1**−**3** Resonances and Their Corresponding Sugar Strand **4**−**6** in D_2O

	Gal $\Delta\delta_H$ [**1**–**4**]	Glc $\Delta\delta_H$ [**2**–**5**]	Xyl $\Delta\delta_H$ [**3**–**6**]
H-1	−0.33	−0.48	−0.31
H-2	−0.07	−0.30	−0.14
H-3	*a*	−0.13	−0.10
H-4	−0.06	−0.12	−0.31
H-5	*a*	−0.06	−0.26
H-5′			−0.29
H-6		−0.10	
H-6′		0	

[a] Overlap.

Table 4. ^{1}H NMR Chemically Induced Shift (CIS) Differences between Sugar−Oligoamide Resonances of **1**−**3** and Their Corresponding Sugar Strands **4**−**6** and Indol Strand **7** in H_2O/[D_6]-Acetone [9:1] for NH Resonances

	Gal $\Delta\delta_H$ [**1**–**4**] $\Delta\delta_H$ [(**1**–**7**)]	Glc $\Delta\delta_H$ [**2**–**5**] $\Delta\delta_H$ [(**2**–**7**)]	Xyl $\Delta\delta_H$ [**3**–**6**] $\Delta\delta_H$ [(**3**–**7**)]
NH^1	(−0.162)	(−0.149)	(−0.107)
NH^2	(−0.210)	(−0.196)	(−0.154)
NH^3	(−0.246)	(−0.241)	(−0.210)
NH^4	0.008	−0.010	0.066
NH^5	−0.205	−0.106	−0.201

All of the sugar pyranose resonances were shielded in the sugar−oligoamides, reflecting their spatial proximity to the indole ring. The anomeric proton resonances present significantly different behaviors in both solvents, depending on the sugar residue. In D_2O/[D_6]-acetone (Table 1) H-1 of the galactose-oligoamide **1** compared with the sugar strand model **4** is +0.019 ppm deshielded. In contrast, the H-1 protons of oligoamides **2** and **3** are shielded. In D_2O (Table 3), the H-1 proton of **1**−**3** is shielded to a similar extent. This suggests either a different relative orientation of the sugar residue with respect to the indole ring or a different degree of hairpin conformation, depending on the solvent. The largest shifts were found for proton resonances of the pyranose rings of Xyl **3**, while the smaller for these particular resonances were observed for Gal **1**.

Table 4 shows the $\Delta\delta$ of the NH resonances of **1**−**3** in H_2O/[D_6]-acetone, in comparison with the corresponding model compounds **4**−**7**.

All NH resonances of **1**−**3** were shielded with respect to the model except NH^4, which shows a very small CIS. In fact, this proton follows a different trend depending on the sugar. Again, these upfield shifts (from −0.106 to −0.246 ppm) are consistent with a folded conformation, in which the aromatic residues of each strand are facing each other, thus affecting the NH resonances. The coupling constant values found in NH^5 resonances for **1**−**3**, and the model compounds **4-6**, which correspond to the proton amide in the sugar anomeric position (9.2−8.5 Hz) (Table D in Supporting Information) are consistent with a trans (180°) or syn (0°) orientation of NH^5 respect to H-1 of the sugar pyranose ring allowing an almost parallel orientation between the plane defined by the sugar pyranose and the indole ring.[35] This is in accordance with the predicted geometry (Figure 2) for the β-anomer sugar−oligoamide hairpin. Based on Avalos et al.[35] there is a preferred anti conformation for structurally similar amido sugars. In our case, the presence of an NOE between NH^5 and H-2 of the pyranose ring and the absence of an NOE between NH^5 and H-1 supports the presence of a major conformation in solution.

In principle, the above-described features in the NMR spectra of **1**−**3** could be additionally due to intermolecular oligomerization, since chemically induced shifts could also be expected for either a head-to-tail dimer or an oligomer of the sugar−amides. We ruled out this possibility, through dilution experiments (in D_2O/[D_6]-acetone and D_2O), which showed that the δ of **1**−**3** did not change in the concentration range from 10 mM to 0.1 mM, where the self-associated oligomers should become less favorable. This confirms that the chemically induced shifts found in the proton resonances of **1**−**3** are due to intramolecular folding. Dilution experiments were also performed in the model compounds **4**−**7** to compare with their corresponding sugar−oligoamides, and with the indole strand acid **7**. Only the acid **7** shows evidence of self-association in D_2O, with a small dimerization constant ($K_a = 100\ M^{-1}$).

The next step was to characterize the geometry of the folded conformation present in solution. With this purpose, NOESY and ROESY experiments were carried out with **1**−**3** in D_2O/[D_6]-acetone, D_2O, and H_2O/[D_6]-acetone solutions. The small intensity of the measured NOEs obtained in D_2O, as well as the strong overlapping of the sugar resonances (mainly in β-Gal-Py-γ-Py-Ind **1** and β-Xyl-Py-γ-Py-Ind **3**), made the structural analysis difficult.

In addition to the γ-linker, several potentially flexible bonds have to be taken in account for structural analysis of **1**−**3**. The conformational preferences around these bonds (Figure 4a) would determine the precise nature of the hairpin structures within the strands. Nevertheless, the experiments in H_2O/[D_6]-acetone allowed tracing the connectivity shown in Figure 4b. Thus, they permitted to unambiguously establish the most populated orientation for these linkages in solution.

These intrastrand NOEs allowed confirming the crescent conformation of the three sugar−oligoamides (**1**−**3**). Similar intrastrand NOEs were described for γ-linked oligoamide covalent dimers in the bound state conformation.[37,46,47]

Particularly interesting is the presence of an NOE between NH^2 and In^3. Thus, the indole In^3 proton is pointing toward the *NH*-amide rim, as suggested by the molecular models. In this sense, the indole residue can be considered as an extended mimic of Py.

Finally, NOESY experiments in D_2O/[D_6]-acetone allowed the determination of the 3D structure of the designed oligoamides in solution.

These experiments showed interstrand NOEs (Table E in the Supporting Information) characteristics of the hairpin conformation, described by Wemmer and co-workers in the bound state for γ-linked oligoamides.[37,46,47]

Thus, spatial proximity among P^{3A}−P^{3B}, P^{5A}−$CH_3{}^B$, and P^{5B}−$CH_3{}^A$ was found in solution in the free state for **1**−**3** (Figure 5), suggesting that the bioactive hairpin structure, previously described for the structurally more complicated minor-groove-DNA-binding Distamycin-type covalent dimers,[37,46,47] is not significantly disturbed by the presence of the sugar moiety. It is remarkable that, in addition to these contacts, unambiguous NOEs between the sugar and the indole ring could be assigned. Thus, NOEs between the indole proton resonances and the sugar pyranose proton resonances present in the β-face of Glc in **2** and Xyl in **3** (Table E in Supporting Information)

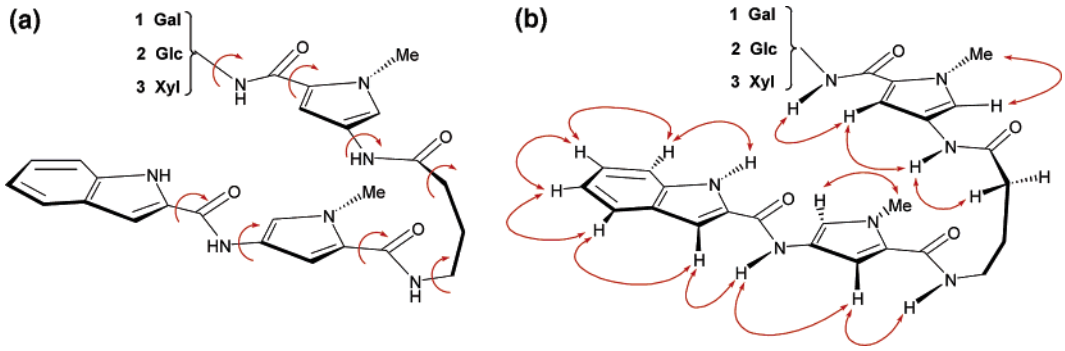

Figure 4. (a) Possible bond rotations of sugar−oligoamide. (b) Intrastrand NOEs found in the NOESY spectra.

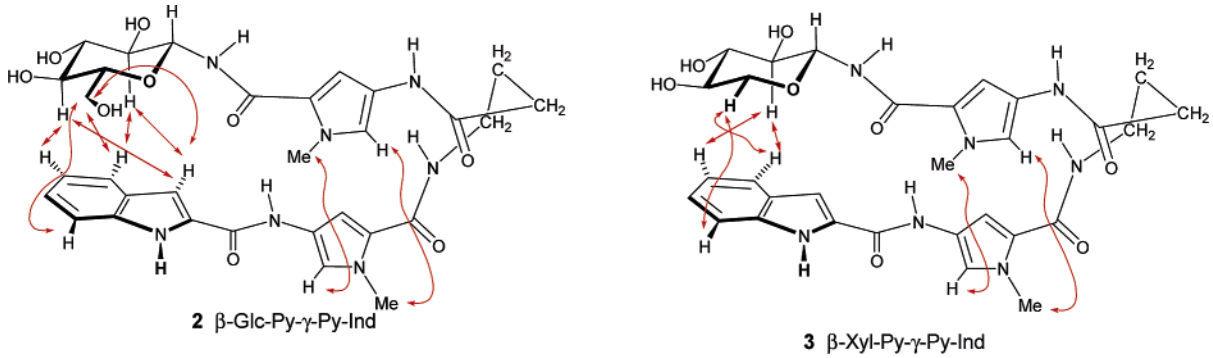

Figure 5. Interstrand NOEs for oligoamides **2** and **3**.

Table 5. ^{1}H NMR Titration of Compounds **1**−**3**, **6**, and **7** with Calf Thymus DNA[a]

	β-Gal-Py-γ-Py-In **1** mM	β-Glc-Py-γ-Py-In **2** mM	β-Xyl-Py-γ-Py-In **3** mM	β-Xyl-Py-NHAc **6** mM	In–Py-γ-OH **7** mM	Netropsin mM
concentration of ct-DNA	2.6	2	0.36	>3.5	>3.5	0.03

[a] Concentration of the solution. Conditions: D_2O, θ = 26 °C, [oligo] =10^{-4} M (0.5 mL), [DNA] =2 mg/0.7 mL

were detected. More specifically, the β-face proton resonances H-2, H-4, and H-6a/H-6b of Glc **2** sugar−oligoamide show clear contacts with In_3, In_4, In_5, and In_7. In a similar way, NOEs between sugar H-2 and H-5_{eq} and In_4, In_5, and In_7 were found for the Xyl **3** derivative. Two different conclusions can be drawn from these results. First, they constitute unequivocal evidence of the presence of a percentage of folded bioactive conformation in aqueous solution. Additionally, it allowed unambiguously defining the precise geometry of the sugar−indole interaction: the aromatic ring mainly stacks against the β-face of the sugar residue.[48] This is similar to that found in the bound state for Dystamicin-type covalent dimer minor groove binders.

Indeed, the conformational analysis of sugar−oligoamides **1**−**3** in the free state shows that the water soluble ligands present a percentage of hairpin conformation in solution in which an *NH*-amide rim and an *N*-methyl rim has been characterized (Figure 6). Regarding the sugar residue, the β-face of the pyranose ring is close to the indole ring in the hairpin conformation. Thus, C-2 and C-3 of the pyranose are pointing to the *NH*-amide rim while C-4, C-5, and O-5 in xylose and C-4, C-5, O-5, and C-6 in glucose are facing the *N*-methyl rim of the sugar−oligoamide.

DNA Interaction. As a further step, we have explored the binding of sugar−oligoamides **1**−**3** to calf-thymus DNA (*ct*-DNA). First, a ^{1}H NMR titration experiment was carried out. Increasing amounts of *ct*-DNA were added to a constant concentration solution of the oligoamide (**1**−**3**). In principle, depending on the kinetics of the free/bound exchange process, DNA binding could affect the chemical shifts, line intensities, and/or the line widths of the ligand resonances. These perturbations can be used to monitor the binding process. Indeed, a significant line broadening of resonances from compounds **1**−**3**, which eventually disappeared below the noise level, is observed upon addition of DNA. Table 5 shows the amount of *ct*-DNA (in base-pair, bp) needed to make disappear from the spectra at least 95% of the resonance signals of the ligand (see Scheme 4).

The sugar−oligoamides **1**−**3** and the model compounds Xyl-Py-NHAc **6** and HO-γ-Py-Ind **7** were used in different binding experiments.

Interestingly, there are significant differences in the amount of *ct*-DNA needed to produce a similar effect on the ligand signals, depending on the nature of the sugar moiety. Indeed, the Xyl-oligoamide **3** proton resonances disappeared from the NMR spectrum upon addition of *ct*-DNA (0.36 mM bp). In contrast, **2** and **1** reached the same situation with much higher concentrations (2 mM and 2.6 mM in bp, respectively). Thus, there is nearly an order of magnitude difference in the required DNA concentration between β-D-Xyl-Py-γ-Py-Ind **3** and β-D-Gal-Py-γ-Py-Ind **1** for the same effect. Although only qualitative, this observation strongly suggests that DNA binding affinity and/or specificity is rather different for ligands **1**, **2**, and **3**. Thus,

(48) Bernardi, A.; Arosio, D.; Potenza, D.; Sanchez-Medina, I.; Mari, S.; Canada, F. J.; Jimenez-Barbero, J. *Chem.−Eur. J.* **2004**, *10*, 4395−4406.

Scheme 4. Titration of **3** with *ct*-DNA.

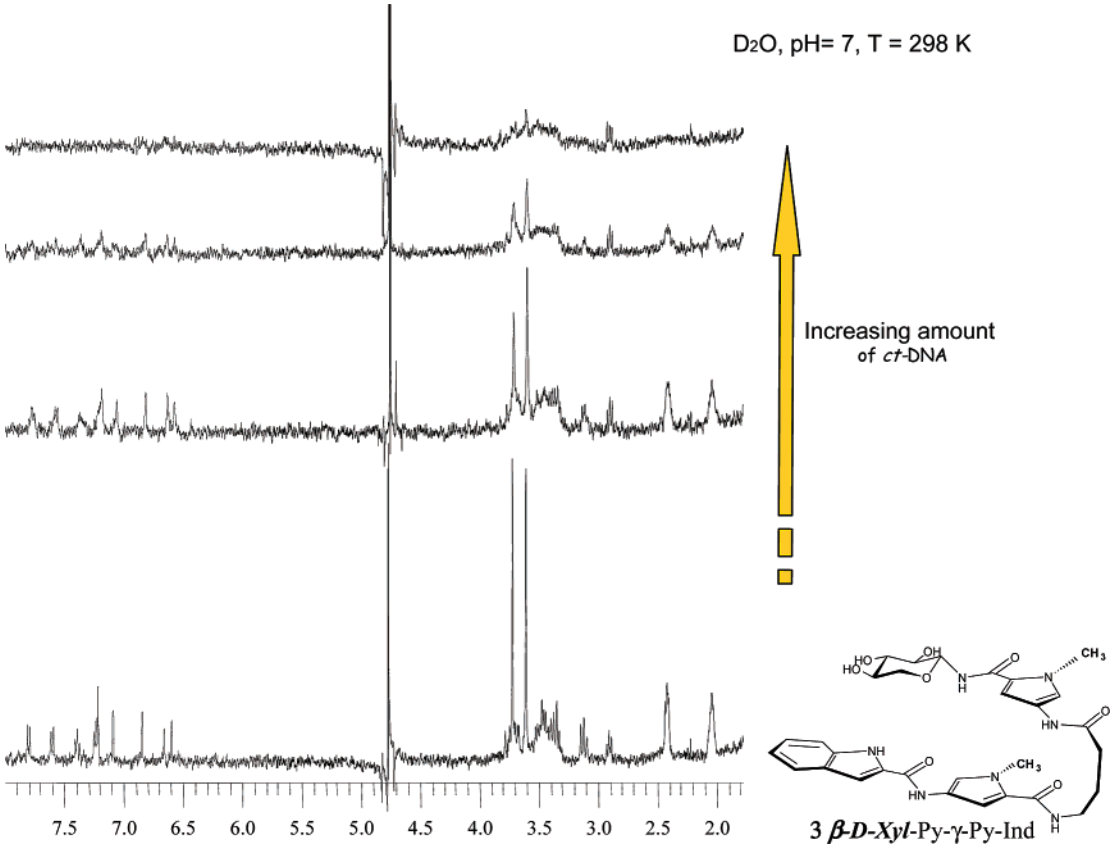

subtle changes on the sugar residue structure may have implications on DNA binding.

There are also differences in the behavior of the individual proton resonances of the sugar−oligoamides upon addition of *ct*-DNA. Thus, proton resonances from the indole moiety and pyrrol (P^{3A} and P^{5A}) are earlier affected (they broaden) upon addition of *ct*-DNA than the rest of them. In contrast, the CH_3 *N*-pyrrol resonances only disappear, below the noise level, after the latest additions of *ct*-DNA and, again, $CH_3{}^A$ does it earlier than $CH_3{}^B$ (see Supporting Information). This general behavior of the three sugar−oligoamides (**1**−**3**) is suggesting that the *NH*-amide rim in the bound state is closer to the *ct*-DNA than the *N*-methyl rim and that the indole strand is closer to the *ct*-DNA than the sugar strand in the bound state (Figure 6). This fact seems to be in agreement with a bound state conformation and binding mode similar to those described for γ-linked oligoamide covalent dimers.[37,46,47]

As a control experiment, two *ct*-DNA titrations were also carried out. In both of them, *O*-methyl-α-D-glucopyranoside, a simple sugar, lacking of the DNA-binding oligoamide linker, was used. The first experiment was a titration experiment in which both sugar−oligoamide β-Glc-Py-γ-Py-Ind **2** and *O*-methyl-α-D-glucopyranoside were present in the same concentration (see Supporting Information). Upon addition of *ct*-DNA at a constant concentration of both substrates, while β-Glc-Py-γ-Py-Ind **2** resonances start to broaden and disappear, the *O*-methyl-α-D-glucopyranoside resonances remained unaffected. As expected, the *O*-methyl-α-D-glucopyranoside is not a DNA substrate. This is probing that the above-mentioned effect observed on **1**−**3** resonance signals upon addition of *ct*-DNA is directly related to DNA binding.

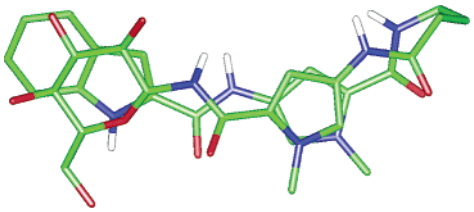

Figure 6. Schematic representation of β-Glc-Py-γ-Py-Ind **2** in solution.

This control experiment was also carried out in an independent manner, by addition of *ct*-DNA to a solution of O-methyl-α-D-glucopyranoside, in the same experimental conditions described for **1**-**3**. Even at high concentrations of DNA (more than 4mM in bp) the *O*-methyl-α-D-glucopyranoside proton resonances did not disappear from the spectra.

Interestingly, under the conditions just mentioned for the sugar−oligoamide titrations, neither the sugar−oligoamide models (**4**−**6**) nor the indole strand acid Ind-Py-γ-COOH (**7**) are DNA binders (after addition of more than 4 mM *ct*-DNA solution the resonances did not disappear from the ^{1}H NMR spectra).

All these evidences are indicating that these isolated fragments (indol strand and the sugar strand) do not show enough contact sites for efficient binding.

As a positive control experiment, the DNA binding experiment was performed using Netropsin as ligand, a well-known effective minor groove binder. It binds *ct*-DNA with a $K_a = 428 \times 10^5\ M^{-1}$.[49]

Thus, a 0.1 mM solution of Netropsin was titrated with a solution of *ct*-DNA which was 30 times more diluted than those

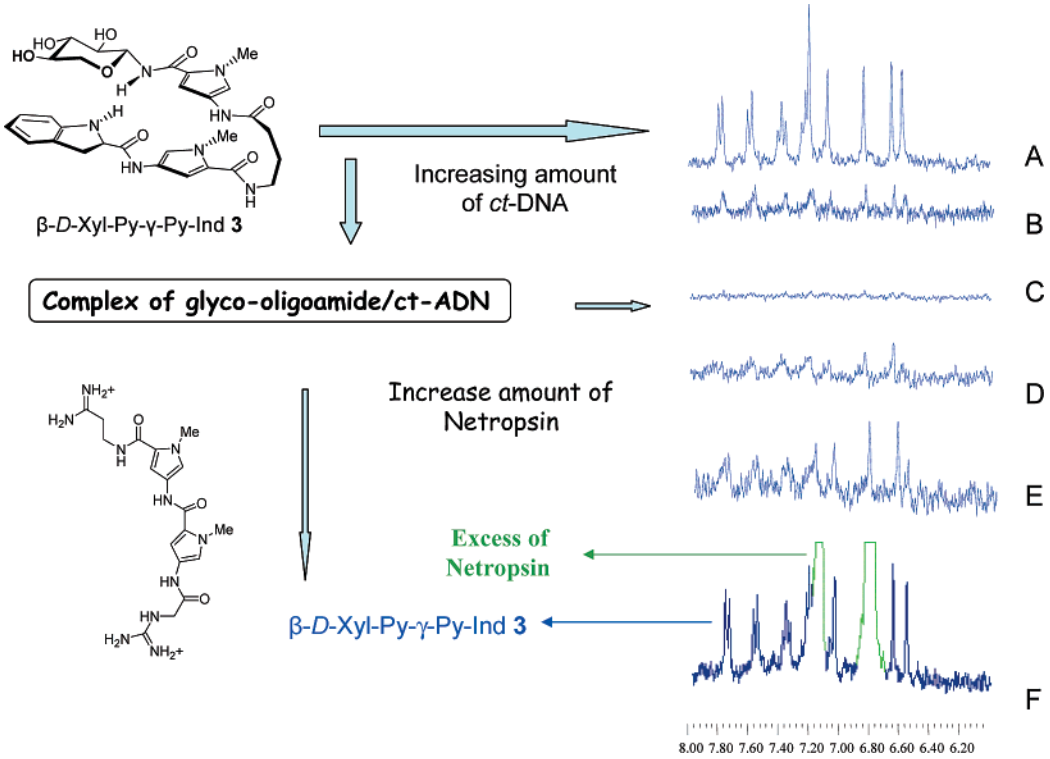

Figure 7. Competition experiment between β-Xyl-Py-γ-Py-Ind **3** and Netropsin; (A) ^{1}H NMR spectra of **3** (0.1mM), (B) **3** in the presence of *ct*-DNA 0.23mM bp, (C) **3** in the presence of *ct*-DNA 0.44mM bp (**3**-*ct*-DNA complex), (D) **3**-*ct*-DNA complex upon addition of Netropsin 0.91mM, (E) **3**-DNA complex upon addition of Netropsin 1.27mM, (F) **3** displaced by Netropsin (2 mM).

used for the sugar−oligoamides. Under that condition, 95% of the proton resonances signals from Netropsin disappear from the spectra upon *ct*-DNA addition (0.03 mM). Thus, there is 1 order of magnitude of difference in the required concentration of DNA needed for the same effect between Netropsin and β-D-Xyl-Py-γ-Py-Ind **3**. This is consistent with an expected more efficient binding of the positively charged ligand Netropsin, compared with our neutral sugar−oligoamides **1**−**3**.[50] Here again, there are also differences in the behavior of the individual proton resonances of the Netropsin upon addition of DNA, and the behavior is similar to that described above for the sugar−oligoamides. Thus, proton resonances from the pyrrol moiety (P^3 and P^5) are affected earlier than the rest of them. In contrast, the CH_3 *N*-pyrrol resonances only disappear, below the noise level, after the latest additions of DNA.

Additionally, an NMR competition experiment was also performed in order to deduce if Netropsin and **3** were sharing common binding sites when interacting with *ct*-DNA. Figure 7 shows the competition experiment following the aromatic resonances of the substrate (between 6.0 and 8.0 ppm).

A 0.1 mM solution of **3** was titrated with *ct*-DNA solution (2 mg/0.7 mL = 3.58 mM en bp) until the resonances from **3** disappeared from the NMR spectra (50 μL, 0.44 mM bp), reflecting the **3**−*ct*-DNA complex formation. Then, a solution of Netropsin (10 mM) was added stepwise to the (**3**−*ct*-DNA) complex. Upon addition of Netropsin (0.91mM and 1.27 mM, see Figure 7), the resonances from the sugar−oligoamide **3** started to appear again in the spectra, thus reflecting the displacement of **3** by Netropsin from the *ct*-DNA binding site.

This experiment shows that the sugar−oligoamide **3** is a minor groove DNA binder that is displaced by Netropsin, suggesting that could share similar binding sites.

The binding experiments of sugar−oligoamides **1** and **3** were also performed with poly(dA-dT) and poly(dG-dC) polynucleotides to obtain information on the sequence selectivity of binding. Additionally, Netropsin was also used as a reference for a structurally related selective minor groove binder. The concentrations (in base pair) of polynucleotide needed to make 95% of the substrate resonances disappear from the ^{1}H NMR spectra are shown in Table F in the Supporting Information.

The comparison of titrations of both sugar−oligoamides **1** and **3** with poly(dA-dT) and poly(dG-dC) shows that the amount of poly(dG-dC) needed to achieve the same effect in the NMR spectra is 4 (for **1**) and 9 (for **3**) times the concentration of poly(dA-dT), respectively. This is suggesting a more efficient binding with poly(dA-dT). The same tendency (10 times) is also found for Netropsin−poly(dA-dT) and poly(dG-dC) titrations but with smaller amounts of macromolecule. In this last case, it is in agreement with the known fact that Netropsin binds preferentially poly(dA-dT) than poly(dG-dC).[51] These results suggest that the positively charged minor groove binder, Netropsin binds an ATAT sequence more effectively than our neutral sugar−oligoamides (**1** and **3**). Nevertheless, our sugar−

(49) Chaires, J. B. *Biopolymers* **1997**, *44*, 201−215.
(50) The reported K_a values are described in experimental conditions not comparable with this NMR titration.
(51) K_a values of Netropsin−poly(dA-dT) = 22 000 × 10^5 M[50,52] and K_a Netropsin−poly(dG-dC) = 1.61 × 10^5 M.[52] It is important to remark that the experimental conditions in which Netropsin−poly(dG-dC) and Netropsin−poly(dA-dT) K_a values are reported are not comparable with our experimental conditions. The lack of salt in our experiments is expected to enhance electrostatic nonspecific interactions. In fact, some extent of nonspecific binding cannot be excluded under these conditions and would explain the small amount of macromolecule concentration needed to achieve binding.

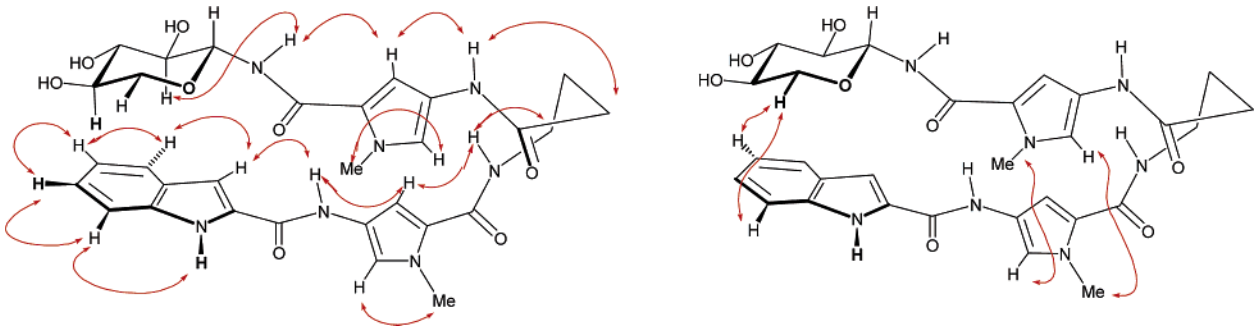

Figure 8. Interstrand and intrastrand NOEs for sugar−oligoamide **3** in the bound state in H_2O/D_2O (15%).

oligoamides (**1** and **3**) present also some preference toward the poly(dA-dT) sequence for binding.

Regarding the comparison between both sugar−oligoamides, β-Gal-Py-γ-Py-Ind **1** needs twice the concentration of poly(dA-dT) than **3**. These results show that ligands β-Gal-Py-γ-Py-Ind **1** and β-Xyl-Py-γ-Py-Ind **3** present a small, but detectable, distinct behavior in binding toward poly(dA-dT) which should be attributed to the differences that the carbohydrate structure (β-Gal and β-Xyl) confers to the general structure of the hairpin ligand.

Finally, TR-NOESY experiments were carried out under different experimental conditions (temperature, ligand/DNA ratio), to analyze the bound state sugar−oligoamide structures in the complexes with *ct*-DNA. The TR-NOESY is a regular NOESY experiment, but it is applied to a big receptor/ligand system in dynamic exchange, in which the ligand is present in excess. In general, for bound ligands, which exchange with the free state at fast rate, exchange transferred (TR-NOE) experiments provide an adequate means to determine the conformation of the bound ligand. In complexes involving large molecules, cross relaxation rates of the bound compound (σ^B) (which depend on the interproton distances of the bound state, the spectrometer frequency, and on the correlation time of the bound ligand) are opposite in sign to those of the free one (σ^F) and produce negative NOEs. Therefore, the existence of binding may be easily deduced from visual inspection, since NOEs for small molecules are positive or close to zero (as **1**−**3**). Because of the relatively low values of cross-relaxation and longitudinal rates in diamagnetic systems ($<10\ s^{-1}$), the experiment is applicable under certain kinetic conditions ($k_{-1} \gg \sigma^B$, where σ^B is the cross relaxation rate for the bound and k_{-1} is the off-rate constant).

Thus, the TR-NOESY experiment in D_2O of compound **3** in the presence of *ct*-DNA was carried out. Negative and intense NOEs were observed, in contrast with the weak positive NOEs which **3** presents in the free state. These TR-NOESY data provide valuable information about the ligand conformation in the bound state. As previously mentioned, the most relevant NOEs, in structural terms, are those that define the hairpin conformation (interstrand NOEs). Thus, clear interstrand contacts between pyrrole A and pyrrole B resonances (NOEs: P^{3A}−P^{3B}, P^{5A}−$CH_3{}^B$, P^{5B}−$CH_3{}^A$) were observed for the sugar−oligoamide **3** (see Supporting Information). This fact conclusively proves that compound **3** is bound to *ct*-DNA and adopts a folded conformation in the bound state, similar to that observed for the free state.

The TR-NOESY in H_2O also shows NOEs in which the cross-peak signs are negative, characteristic of binding (see Supporting Information). Even more relevant, the NOEs between the N−H amide resonances and the next amino acid residue resonances (intrastrand) confirmed that the conformation in the bound state presents an N−H rim and CH_3 rim, as detected for the free ligand (see Figure 8). In this experiment, pyrrol−pyrrol interstrand NOEs (see Figure 8) were also detected. Additionally, NOEs between the sugar β-face proton resonances and the indol ring (NOEs H-5_{eq}-In^6 and H-5_{eq}-In^4) were detected, which suggests that the sugar−oligoamide hairpin bound state conformation also places the sugar β-face close to the indol ring. Thus, regarding the sugar unit, the C-2 and C-3 positions are directed to the *NH*-amide rim, while C-4, O-5, C-5, and C-6 are pointing toward the *N*-methyl rim of the sugar−oligoamide (see Figure 9).

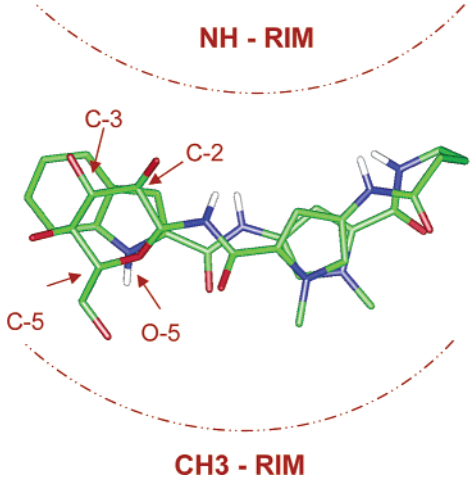

Figure 9. Schematic representation of β-Glc-Py-γ-Py-Ind **2** in the bound state.

Conclusions

Sugar−oligoamides have been designed and synthesized. The major aim of this work is to be able to position a structurally simple monosaccharide at close distance of the DNA minor groove. Thus, the smallest oligoamide fragment resembling the known Distamicin-type γ-linked oligoamide dimers has been selected. It was expected that this design would help the hairpin conformation (bound state conformation) to be locked in the free state by $\pi-\pi$ interactions and CH−π interactions between the indol moiety and the sugar pyranose ring.

Indeed, the conformational analysis of sugar−oligoamides **1**−**3** in the free state shows that these water soluble carbohydrate ligands present a certain percentage of hairpin conformation in solution, in which an *N*−*H* amide rim and an *N*-methyl rim have been characterized. The sugar places its β-face close to the indole ring in the adopted hairpin conformation. Thus, C-4,

O-5, C-5, and C-6 of the pyranose are in the *N*-methyl rim, while C-2 and C-3 of the pyranose are pointing toward the *N*−*H* amide rim of the sugar−oligoamide.

The ability of the ligands to bind *ct*-DNA has been shown qualitatively by ^{1}H NMR titration, following the disappearance of the ligand resonance signals upon increasing addition of *ct*-DNA. This method has allowed us to show that **1**−**3** are *ct*-DNA binders while Ind-Py-γ- COOH **7** or sugar-Py-NHAc **4**−**6** are not ligands in the same conditions. The well-known structurally related Netropsin minor groove binder has also been tested by this method, as a control experiment.

The results from the binding experiments suggest, although only qualitatively, that DNA binding affinity and/or specificity is different for the three ligands. Thus, subtle changes on the sugar residue structure may have implications on DNA binding. β-Xyl-Py-γ-Py-Ind **3** seems to be the best sugar−oligoamide *ct*-DNA binder.

Additionally, a competition experiment followed by ^{1}H NMR between our sugar−oligoamide from xylose **3** and Netropsin has shown that Netropsin is able to displace **3** from its complex with *ct*-DNA, suggesting that **3** is a minor groove binder.

We have also used the ^{1}H NMR titrations to explore sequence selectivity of binding for sugar−oligoamides **1** and **3** toward poly (dA-dT) and poly (dG-dC). Comparisons have also been made with Netropsin in the same conditions. Interestingly, both Gal **1** and Xyl **3** sugar−oligoamide seem to present a preference of binding toward the ATAT sequence rather than to GCGC.

The most relevant result is that TR-NOESY experiments in D_2O and H_2O of xylose sugar−oligoamide **3** in the presence of *ct*-DNA have confirmed that the designed carbohydrate ligands bind *ct*-DNA (a change in the sign of the NOEs from free to bound) and the bound conformation presents the same intra- and interstrand NOEs as those observed in the free state. This is suggesting that the sugar−oligoamides bind *ct*-DNA in a hairpin conformation similar to that found in the free state. More relevant, the carbohydrate residue places the pyranose ring C-4, C-5, O-5 and C-6 directed to the *N*-methyl rim while C-2 and C-3 of the pyranose are pointing toward the *NH*-amide rim of the sugar−oligoamide (see Figure 9). This structural information of the bound state conformation will be very relevant to the future design of a sugar residue with particular cooperative HB motives directed to the minor groove H-bonding centers.[19,20,52]

Experimental Section

General. Solvents were purified according to the standard procedures. Melting points are reported in degrees Celcius (uncorrected) with a microscope Reicher Jung Thermovar. NMR measurements were recorded on a Varian Gemini-200 (200 MHz), Varian Inova-300 (300 MHz), Varian Inova-400 (400 MHz), Varian Unity-500 (500 MHz), and Bruker AVANCE 500 MHz spectrometers. Mass spectrometry analyses were performed with an HP series 1100 MSD. Optical rotations were measured on a Perkin-Elmer 241MC polarimeter in a 1 dm cell. Elemental analyses were measured on a Carla Erba CHNS-O EA1108 chromatography system. Thin-layer chromatography was performed on silica gel on aluminum sheets 60F_{254} (Merck). Flash chromatography was performed on silica gel 60 (0.040−0.063 mm) (Merck).

Calf thymus DNA (*ct*-DNA) was purchased from Sigma (Lot 90k7063) and used without further purification. *O*-Methyl-α-D-glucopyranoside was purchased from Aldrich (Lot 17602−055). H_2O for NMR studies was freshly filtered milli-q water.

Synthesis Section. β-Gal-Py-γ-Py-Ind (1). A solution of **(AcO)$_4$-β-Gal-Py-γ-Py-Ind 1(OAC)** (92.0 mg, 0.112 mmol) in MeOH (5 mL) was treated with a solution of sodium (100 mg, 4.34 mmol) in MeOH (10 mL) to produce an immediate deeper yellow color, indicative of reaction to completion. The solution was acidified to pH = 6 with Amberlite IR-120 ion-exchange resin (strongly acidic), and the resin was removed by filtration. Evaporation of the solvent under reduced pressure afforded the title compound as an off-white solid (40.0 mg, 53%). This hygroscopic residue was dissolved in MeOH (5 mL) and treated with enough Et_2O to cause a white precipitate to form, which was removed by filtration and dried under vacuum at 40 °C to produce an analytical sample. Mp = 200 °C; IR (KBr): ν = 3600−2500, 1643, 1584, 1530 cm^{-1}; $[\alpha]^{D}_{22}$ = +23.7 (c = 1.35 in [D_6] DMSO). ^{1}H NMR (400 MHz, [D_6] DMSO): δ = 1.79 (m, 2H), 2.28 (m, 2H), 3.22 (m, 2H), 3.30−3.54 (m, 3H), 3.57−3.64 (m, 2H), 3.70 (d, J = 2.7 Hz, 1H), 3,79 (s, 3H), 3.84 (s, 3H), 4.83 (t, J = 8.9 Hz, 1H), 6.85 (d, J = 1.7 Hz, 1H), 6.89 (d, J = 1.7 Hz, 1H), 7.05 (t, J = 8.0 Hz, 1H), 7.20 (m, 2H), 7.28 (s, 2H), 7.53 (d, J = 8.2 Hz, 1H), 7.64 (d, J = 8.2 Hz, 1H), 8.12 (t, J = 5.7 Hz, 1H), 8.36 (d, J = 8.8 Hz, 1H), 9.83 (s, 1H), 10.30 (s, 1H), 11.61 (d, J = 1.5 Hz, 1H). ^{13}C NMR (50 MHz, [D_6] DMSO): δ = 25.6, 33.3, 36.0, 36.1, 38.2, 60.4, 66.3, 69.1, 74.3, 76.6, 80.1, 102.8, 104.1, 104.5, 112.2, 118.0, 118.4, 119.6, 121.4, 121.5, 121.8, 122.2, 123.2, 127.0, 131.5, 136.5, 141.3, 158.1, 161.1, 161.1, 169.2. MS (ES+): m/z (%): 1304 (6) [2M + H]$^+$, 675 (43) [M + Na]$^+$, 653 (100) [M + H]$^+$. Elemental analysis calcd (%) for $C_{31}H_{37}N_7O_9\cdot 2H_2O$ (687.7): C, 54.14; H, 6.01; N, 14.26. Found: C, 54.45; H, 6.02; N, 14.35.

(AcO)$_4$-β-Gal-Py-γ-Py-Ind [1(OAc)]. A solution of **(AcO)$_4$-β-Gal-Py-NO$_2$ 9** (200 mg, 0.400 mmol) in MeOH (5 mL) and EtOAc (5 mL) was treated with 10% Pd−C (40 mg, 9 mol %) under H_2, 45 psi for 24 h. Once the reaction was finished, the catalyst was removed by filtration and the solvent evaporated under reduced pressure to afford a pale brown glassy film which corresponds to the amino derivative of **9**. Separately, a solution of DIPC (63.0 μL, 0.400 mmol), HOBt (54.0 mg, 0.400 mmol), and **HO-γ-Py-Ind 7** (147 mg, 0.400 mmol) in DMF (10 mL) was stirred under argon at room temperature during 24 h before addition of the solution of the amino derivative of **9** in DMF (5 mL). After 24 h under these conditions, the solvent was evaporated and the residue was purified by repeated column chromatography (SiO_2, EtOAc, then SiO_2, 10% MeOH in CH_2Cl_2) to afford an analytical sample of **(AcO)$_4$-Gal-Py-γ-Py-Ind 1(OAc)** as an amorphous white solid (140 mg, 43%). Mp = 165−167 °C. IR (KBr): ν = 1748, 1646, 1531, 1248, 1232 cm^{-1}. $[\alpha]^{D}_{23}$ = +0.926 (c = 3.09 in acetone). ^{1}H NMR (500 MHz, [D_6] DMSO): δ = 1.80 (t, J = 7.5 Hz, 2H), 1.91 (s, 3H), 1.92 (s, 3H), 1.99 (s, 3H), 2.12 (s, 3H), 2.29 (t, J = 7.5 Hz, 2H), 3.23 (m, J = 6.0 Hz, 2H), 3.78 (s, 3H), 3.84 (s, 3H), 4.02 (m, 2H), 4.32 (t, J = 6.0 Hz, 1H), 5.22 (t, J = 9.3 Hz, 1H), 5.30 (m, 2H), 5.45 (t, J = 9.3 Hz, 1H), 6.78 (s, 1H), 6.90 (s, 1H), 7.05 (t, J = 7.5 Hz, 1H), 7.20 (t, J = 7.8 Hz, 1H), 7.24 (s, 1H), 7.28 (s, 2H), 7.46 (d, J = 8.0 Hz, 1H), 7.65 (d, J = 8.0 Hz, 1H), 8.07 (m, 1H), 8.74 (d, J = 9.5 Hz, 1H), 9.82 (s, 1H), 10.30 (s, 1H), 11.58 (s, 1H). ^{13}C NMR (125 MHz, [D_6] DMSO): δ = 20.3, 20.4, 20.4, 20.4, 25.6, 33.2, 36.0, 36.1, 38.2, 61.4, 67.6, 68.3, 71.1, 71.3, 77.5, 102.8, 104.1, 104.9, 112.2, 118.0, 119.2, 119.7, 121.5, 121.5, 121.6, 122.1, 123.3, 123.3, 127.1, 131.6, 136.5, 158.2, 160.9, 161.2, 169.0, 169.3, 169.4, 169.8, 169.9. MS (ES+) m/z (%): 1663 (8) [2M + Na]$^+$, 1641 (4) [2M + H]$^+$, 843 (89) [M + Na]$^+$, 821 (100) [M + H]$^+$. Elemental analysis calcd (%) for $C_{39}H_{45}N_7O_{13}$ (819.8): C, 57.14; H, 5.53; N, 11.96. Found: C, 56.78; H, 5.60; N, 11.69.

β-Glc-Py-γ-Py-Ind (2). Prepared as mentioned above for **β-Gal-Py-γ-Py-Ind 1**, using a solution of **(AcO)$_4$-β-Glc-Py-γ-Py-Ind 2(OAc)**

(52) Vicente, V.; Martin, J.; Jiménez-Barbero, J.; Chiara, J.-L.; Vicent, C. *Chem.−Eur. J.* **2004**, *10*, 4240−4251.

(53) Marky, L. A.; Breslauer, K. J. *Proc. Natl. Acad. Sci.* **1987**, *84*, 4359−4363.

(100 mg, 0.122 mmol) in MeOH (10 mL) and 2 mL of a solution of sodium (100 mg, 4.34 mmol) in MeOH (10 mL) to afford the title compound as a yellow film (33.0 mg, 42%). An analytical sample was prepared by precipitation from a solution in $CHCl_3$ (10 mL) and MeOH (5 mL) with Et_2O, which gave **2** as an amorphous white solid. Mp = 196−197 °C. IR (KBr): ν = 3600−2800, 1638, 1584, 1532 cm^{-1}. $[\alpha]^D_{27}$ = +12.9 (c = 0.760 in [D_6] DMSO). ^{1}H NMR (200 MHz, [D_6] DMSO): δ = 1.79 (m, 2H), 2.29 (m, 2H), 3.21 (m, 2H), 3.64 (m, 1H), 3.79 (s, 3H), 3.84 (s, 3H), 4.51 (t, J = 5.7 Hz, 1H), 4.81 (d, J = 5.3 Hz, 1H), 4.87 (d, J = 4.4 Hz, 1H), 4.96 (d, J = 4.0 Hz, 1H), 6.85 (d, J = 1.7 Hz, 1H), 6.90 (d, J = 1.7 Hz, 1H), 7.06 (m, 1H), 7.19 (m, 2H), 7.28 (s, 2H), 7.46 (d, J = 8.2 Hz, 1H), 7.65 (d, J = 7.9 Hz, 1H), 8.13 (t, J = 4.9 Hz, 1H), 8.36 (d, J = 8.8 Hz, 1H), 9.82 (s, 1H), 10.29 (s, 1H), 11.60 (s, 1H). ^{13}C NMR (200 MHz, DMSO): 25.6, 33.2, 33.5, 35.8, 36.0, 61.0, 70.1, 71.8, 77.6, 78.4, 79.4, 79.6, 103.2, 104.1, 112.5, 118.2, 119.6, 121.5, 121.5, 121.8, 122.2, 123.2, 123.2, 127.0, 127.0, 131.6, 161.1, 161.1, 169.6. MS (ES+) m/z (%): 1325 (9) $[2M + Na]^+$, 1304 (3) $[2M + Na]^+$, 674 (90) $[M + Na]^+$, 652 (100) $[M + H]^+$. Elemental analysis calcd (%) for $C_{31}H_{37}N_7O_9$ (651.7): C, 57.14; H, 5.72; N, 15.05. Found: C, 57.19; H, 5.68; N, 15.1.

(AcO)$_4$-β-Glc-Py-γ-Py-Ind [2(OAc)]. Prepared as mentioned above for **1(OAc)**, using a solution of **(AcO)$_4$-β-Glc-Py-NO$_2$ 10** (500 mg, 1.00 mmol). Compound **(AcO)$_4$-Glc-Py-γ-Py-Ind 2(OAc)** obtained as an amorphous white solid (450 mg, 55%). Mp = 160−161 °C; IR (KBr): ν = 1749, 1645, 1234 cm^{-1}. $[\alpha]^D_{25}$ = +10.6 (c = 1.56 in [D_6] DMSO). ^{1}H NMR (400 MHz, [D_6] DMSO): δ = 1.80 (m, 2H), 1.90 (s, 3H), 1.94 (s, 3H), 1.99 (s, 3H), 2.00 (s, 3H), 2.28 (t, J = 7.4 Hz, 2H), 3.23 (m, 2H), 3.79 (s, 3H), 3.84 (s, 3H), 4.00 (dd, J = 1.9 Hz, 12.3 Hz, 1H), 4.10 (ddd, J = 2.1 Hz, 4.3 Hz, 10.0 Hz, 1H), 4.19 (dd, J = 4.5 Hz, 12.4 Hz, 1H), 4.91 (dd, J = 9.7 Hz, 9.9 Hz, 1H), 5.09 (dd, J = 9.3 Hz, 9.5 Hz, 1H), 5.36 (dd, J = 9.5 Hz, 9.7 Hz, 1H), 5.50 (dd, J = 9.3 Hz, 9.5 Hz, 1H), 6.77 (d, J = 2.0 Hz, 1H), 6.90 (d, J = 1.8 Hz, 1H), 7.06 (m, 1H), 7.17−7.23 (m, 2H), 7.28 (m, 2H), 7.46 (dd, J = 0.9 Hz, 8.2 Hz, 1H), 7.65 (d, J = 7.9 Hz, 1H), 8.09 (dd, J = 5.5 Hz, 5.9 Hz, 1H), 8.66 (d, J = 9.5 Hz, 1H), 9.84 (s, 1H), 10.27 (s, 1H), 11.59 (d, J = 1.8 Hz, 1H). ^{13}C NMR (100 MHz, [D_6] DMSO): δ = 20.3, 20.3, 20.5, 25.6, 33.2, 36.0, 36.1, 38.2, 61.7, 67.9, 70.6, 72.0, 73.1, 77.2, 79.1, 102.8, 104.1, 104.9, 112.3, 118.1, 119.2, 119.8, 121.4, 121.5, 121.6, 122.2, 123.3, 123.4, 127.1, 127.1, 136.6, 158.2, 160.9, 161.2, 169.0, 169.3, 169.3, 169.5, 170.0. MS (ES+) m/z (%): 1662 (1) $[2M + H]^+$, 842 (22) $[M + Na]^+$, 820 (79) $[M + H]^+$, 410 (100) [(AcO)$_3$-Glc-Py-NH$^-$]. Elemental analysis calcd (%) for $C_{39}H_{45}N_7O_{13}$ + 1.2H_2O (841.4): C, 55.67; H, 5.68; N, 11.65. Found: C, 55.42; H, 5.49; N, 11.44.

β-Xyl-Py-γ-Py-Ind (3). Prepared as described above for **1** using a solution of **(AcO)$_3$-β-Xyl-Py-γ-Py-Ind 3 (OAc)** (100 mg, 0.133 mmol) in MeOH (10 mL) and 2 mL of a solution of sodium (100 mg, 4.34 mmol) in MeOH (10 mL). The product was purified by column chromatography (EtOAc/MeOH 8:2) and afforded three fractions. The α anomer of **Xyl-Py-γ-Py-Ind** (15.5 mg, 19%), the β anomer of **Xyl-Py-γ-Py-Ind 3** (27.2 mg, 33%), and a mixture of both anomer α/β **of Xyl-Py-γ-Py-Ind** (23.3 mg, 29%) were obtained.

β-Xyl-Py-γ-Py-Ind 3: R_f = 0.40 (EtOAc/MeOH 7:3 v/v). $[\alpha]^D_{22}$ = +5.5 (c = 1 in DMSO). ^{1}H NMR (400 MHz, [D_6] DMSO): δ = 1.79 (m, 2H, CH_2), 2.28 (t, J = 7.6 Hz, 2H, CH_2), 3.04 (t, J = 10.8 Hz, 2H, CH_2), 3.10−3.36 (m, 4H, 4CH), 3.65 (m, 1H, CH), 3.77 (s, 3H, CH_3), 3.83 (s, 3H, CH_3), 4.77 (t, J = 8.8 Hz, 1H, CH1), 4.86 (d, J = 5.6 Hz, 1H, OH), 4.95 (d, J = 5.2 Hz, 1H, OH), 5.04 (d, J = 4.8 Hz, 1H, OH), 6.83 (d, J = 1.6 Hz, 1H, CH), 6.89 (d, J = 2.0 Hz, 1H, CH), 7.05 (dd, J = 6.8 Hz, 8.0 Hz, 1H, CH), 7.17−7.21 (m, 2H, 2CH), 7.28 (d, J = 1.6 Hz, 2H, 2CH), 7.45 (d, J = 8.4 Hz, 1H, CH), 7.64 (d, J = 8.0 Hz, 1H, CH), 8.12 (t, J = 5.6 Hz, 1H, NH3), 8.35 (d, J = 8.8 Hz, 1H, NH5), 9.83 (s, 1H, NH4), 10.31 (s, 1H, NH2), 11.62 (s, 1H, NH1). ^{13}C NMR (500 MHz, [D_6] DMSO): δ = 26.6 (CH_2), 33.2 (CH_2), 35.9 (CH_3py), 36.1 (CH_3py), 38.2 (CH_2), 67.3 (CH_2), 69.7 (CH), 71.6 (CH), 77.6 (CH), 80.5 (CH), 102.8 (CH), 104.1 (CH), 104.6 (CH), 112.3 (CH), 118.1 (CH), 118.5 (CH), 119.7 (CH), 121.5 (CH), 121.6 (C), 121.9 (C), 122.2 (C), 123.2 (C), 123.3 (CH), 127.1 (C), 131.6 (C), 136.5 (C), 158.2 (C), 161.2 (C), 161.3 (C), 169.2 (C). MS (ES+) m/z (%): 1243 (5.8) $[2M + H]^+$, 644 (19.2) $[M + Na]^+$, 622 (100) $[M + H]^+$ $]^+$. Elemental analysis calcd (%) for $C_{30}H_{35}N_7O_8$ (621.64): C, 57.96; H, 5.67; N, 15.77. Found: C, 57.89; H, 5.68; N, 15.69.

The α anomer of **Xyl-Py-γ-Py-Ind**: R_f = 0.59 (EtOAc/MeOH 7:3 v/v). $[\alpha]^D_{23}$ = −7.8 (c = 0.11 in methanol). ^{1}H NMR (400 MHz, [D_6] DMSO): δ = 1.79 (m, 2H, CH_2b), 2.28 (t, J = 7.4 Hz, 2H, CH_2a), 3.21 (m, 2H, CH_2c), 3.30−3.76 (m, 5H, 5CH), 3.77 (s, 3H, CH_3^A), 3.83 (s, 3H, CH_3^B), 4.98 (s, 1H, OH), 5.04 (s, 1H, OH), 5.17 (s, 1H, OH), 5.36 (dd, J = 8.4 Hz, 3.2 Hz, 1H, CH1), 6.80 (d, J = 1.6 Hz, 1H, CH), 6.89 (d, J = 1.6 Hz, 1H, CH), 7.05 (dd, J = 7.2 Hz, 8.0 Hz, 1H, CH), 7.17−7.21 (m, 2H, 2CH), 7.28 (d, J = 1.2 Hz, 2H, 2CH), 7.45 (d, J = 8.4 Hz, 1H, CH), 7.64 (d, J = 8.0 Hz, 1H, CH), 7.70 (d, J = 8.8 Hz, 1H, NH5), 8.11 (t, J = 5.6 Hz, 1H, NH3), 9.81 (s, 1H, NH4), 10.32 (s, 1H, NH2), 11.65 (s, 1H, NH1). ^{13}C NMR (300 MHz, [D_6] DMSO): δ = 21.7 (CH_2), 33.3 (CH_2), 36.1 (2CH_3), 38.2 (CH_2), 64.9 (CH_2), 68.8 (CH), 70.5 (CH), 70.6 (CH), 75.8 (CH), 102.9 (CH), 104.1 (CH), 104.6 (CH), 112.3 (CH), 118.1 (CH), 118.6 (C), 119.8 (CH), 121.5 (CH), 121.6 (CH), 122.0 (C), 122.1 (C), 123.2 (C), 123.4 (CH), 127.1 (C), 131.7 (C), 136.6 (C), 158.2 (CO), 161.1 (CO), 161.2 (CO), 169.3 (CO). MS (ES+) m/z (%): 1265 (14) $[2M + Na]^+$, 644 (41) $[M + Na]^+$, 622 (100) $[M + H]^+$. Elemental analysis calcd (%) for $C_{30}H_{35}N_7O_8$ (621.64): C, 57.96; H, 5.67; N, 15.77. Found: C, 57.99; H, 5.75; N, 15.81.

(AcO)$_3$-β-Xyl-Py-γ-Py-Ind [3(OAc)]. **(AcO)$_3$-β-Xyl-Py-γ-Py-Ind 3(OAc)** was prepared as described above for **1(OAc)** using a solution of a mixture of α and β anomers of **(AcO)$_3$-Xyl-Py-NO$_2$** (365 mg, 0.854 mmol) in CH_2Cl_2 (10 mL) with 10% Pd−C (45 mg) (H_2, atm pressure, 20 h). A mixture of both anomers of **(AcO)$_4$-Xyl-Py-γ-Py-Ind** as a gum was contained (α:β = 1:2) (269 mg, 48%). An analytical sample of the β-isomer was separated and characterized.

(AcO)$_3$-β-Xyl-Py-γ-Py-Ind 3(OAc): R_f = 0.58 (EtOAc/MeOH 9:1 v/v); ^{1}H NMR (200 MHz, [D_6] DMSO): δ = 1.79 (m, 2H, CH_2b), 1.91 (s, 3H, CH_3), 1.97 (s, 3H, CH_3), 2.00 (s, 3H, CH_3), 2.27 (m, 2H, CH_2a), 3.21 (m, 2H, CH_2c), 3.56 (m, 1H, CH), 3.77 (s, 3H, CH_3^A), 3.83 (s, 3H, CH_3^B), 3.89 (m, 1H, CH), 4.81 (m, 1H, CH), 5.06 (dd, J = 9.2 Hz, 9.4 Hz, 1H, CH1), 5.30 (m, 2H, 2CH), 6.72 (d, J = 1.4 Hz, 1H, CH), 6.89 (d, J = 1.8 Hz, 1H, CH), 7.04 (dd, J = 7.8 Hz, 7.2 Hz, 1H, CH), 7.20 (m, 2H, 2CH), 7.27 (s, 2H, 2CH), 7.45 (d, J = 8.0 Hz, 1H, CH), 7.64 (d, J = 7.8 Hz, 1H, CH), 8.10 (m, 1H, NH3), 8.58 (d, J = 9.2 Hz, 1H, NH5), 9.85 (s, 1H, NH4), 10.28 (s, 1H, NH2), 11.60 (s, 1H, NH1). ^{13}C NMR (200 MHz, [D_6] DMSO): δ = 20.2 (3CH_3), 25.5 (CH_2), 33.2 (CH_2), 35.8 (2CH_3), 38.1 (CH_2), 63.2 (CH), 68.6 (CH), 70.6 (CH), 72.7 (CH), 77.6 (CH), 102.7 (CH), 104.1 (CH), 104.8 (CH), 112.1 (CH), 118.0 (CH), 118.9 (CH), 119.6 (CH), 121.5 (CH), 121.9 (3C), 122.0 (C), 123.2 (CH), 127.0 (C), 131.6 (C), 136.5 (C), 158.1 (HNCO), 160.9 (HNCO), 161.1 (HNCO), 168.9 ($COCH_3$), 169.2 ($COCH_3$), 169.4 ($COCH_3$). MS (ES+) m/z (%): 1517 (8) $[2M + Na]^+$, 1495 (10) $[2M + H]^+$, 770 (30) $[M + Na]^+$, 748 (100) $[M + H]^+$.

The α anomer of **(AcO)$_3$-Xyl-Py-γ-Py-Ind** could not be purified. The mixture of α and β anomers **(AcO)$_3$-Xyl-Py-γ-Py-Ind** showed the ^{1}H NMR as follows: ^{1}H NMR (200 MHz, [D_6] DMSO): δ = 1.79 (m, 4H, CH_2bα, CH_2bβ), 1.91 (s, 3H, $CH_3\beta$), 1.97 (s, 3H, $CH_3\beta$), 1.98 (s, 3H, $CH_3\alpha$), 2.00 (s, 3H, $CH_3\beta$), 2.01 (s, 3H, $CH_3\alpha$), 2.04 (s, 3H, $CH_3\alpha$), 2.28 (m, 4H, CH_2cα, CH_2cβ), 3.23 (m, 4H, CH_2aα, CH_2aβ), 3.56 (m, 2H, 2CHβ), 3.75 (s, 3H, $CH_3^P\alpha$), 3.77 (s, 3H, $CH_3^P\beta$), 3.83 (s, 6H, $CH_3^P\alpha$, $CH_3^P\beta$), 4.83 (m, 5H, 4CHα, CHβ), 5.05 (t, J = 9.4 Hz, 1H, CHβ), 5.32 (m, 2H, 2CHβ), 5.74 (m, 2H, 2CHα), 6.72 (d, J = 1.8 Hz, 2H, $CH^P\alpha$, $CH^P\beta$), 6.89 (d, J = 1.6 Hz, 2H, $CH^P\alpha$, $CH^P\beta$), 6.95 (d, J = 1.8 Hz, 2H, CHα, CHβ), 7.05 (dd, J = 7.0 Hz, 6.8 Hz, 2H, CHα, CHβ), 7.20 (m, 4H, 4CH$\alpha\beta$), 7.28 (s, 2H, CHα, CHβ), 7.45 (d, J = 8.2 Hz, 2H, CHα, CHβ), 7.65 (d, J = 8.2 Hz, 2H, CHα, CHβ), 8.11 (br, 2H, NH3α, NH3β), 8.59 (d, J = 9.6 Hz, 1H, NH5β), 8.79 (d,

J = 9.2 Hz, 1H, NH5α), 9.85 (s, 2H, NH4α, NH4β), 10.29 (s, 2H, NH2α, NH2β), 11.61 (s, 2H, NH1α, NH1β).

β-Gal-Py-NHAc (4). A solution of **(AcO)$_4$-β-Gal-Py-NHAc 17** (80.0 mg, 0.156 mmol) in MeOH (5 mL) was added to a solution of sodium (100 mg, 4.34 mmol) in MeOH (10 mL) to afford the title compound as a colorless film that crystallizes from the crude mixture by Et_2O addition (44.0 mg, 82%). Mp = 148−149 °C; $[\alpha]^D_{22} = -2.6$ (c = 1 in H_2O). ^{1}H NMR (400 MHz, [D$_6$] DMSO): δ = 1.95 (s, 3H), 3.30−3.44 (m, 3H), 3.49 (m, 1H), 3.59 (dd, J = 9.2 Hz, 9.2 Hz, 1H), 3.70 (d, J = 3.1 Hz, 1H), 3.78 (s, 3H), 4.83 (m, 1H), 6.84 (d, J = 1.8 Hz, 1H), 7.16 (d, J = 1.8 Hz, 1H), 8.36 (d, J = 9.2 Hz, 1H), 9.80 (s, 1H); ^{13}C NMR (300 MHz, [D$_6$] DMSO): δ = 23.0, 36.3, 54.9, 60.5, 68.3, 69.1, 74.4, 76.7, 80.1, 104.4, 118.4, 122.0, 161.3, 166.5. MS (ES+) m/z (%): 709 (34) $[2M + Na]^+$, 687 (19) $[2M + H]^+$, 453 (37), 366 (19) $[M + Na]^+$, 344 (100) $[M + H]^+$, 182 (18).

β-Glc-Py-NHAc (5). Prepared as described above for **4**, from a solution of **(AcO)$_4$-β-Glc-Py-NHAc 18** (110 mg, 0.215 mmol) in MeOH. Precipitation from the MeOH solution with Et_2O afforded an analytical sample of the title compound as an amorphous white solid (61 mg, 83%). Mp = 161−163 °C; IR (KBr): ν = 3600−3200, 1644 cm^{-1}. $[\alpha]^D_{27} = +18.6$ (c = 1.37 in [D$_6$] DMSO). ^{1}H NMR (300 MHz, [D$_6$] DMSO): δ = 1.96 (s, 3H), 3.04−3.15 (m, 2H), 3.21 (dd, J = 8.1 Hz, 8.8 Hz, 1H), 3.31 (dd, J = 8.8 Hz, 9.0 Hz, 1H), 3.40−3.67 (m, 2H), 3.79 (s, 3H), 4.88 (dd, J = 8.8 Hz, 9.0 Hz, 1H), 6.83 (d, J = 1.8 Hz, 1H), 7.14 (d, J = 1.8 Hz, 1H), 8.33 (d, J = 8.9 Hz, 1H), 9.77 (s, 1H). ^{13}C NMR (50 MHz, [D$_6$] DMSO): δ = 22.9, 36.0, 61.0, 70.1, 71.8, 77.6, 78.4, 79.6, 104.5, 118.3, 121.9, 122.2, 161.1, 166.4. MS (ES+) m/z (%): 739 (21) $[2M + K]^+$, 709 (100) $[2M + H]^+$, 374 (18) $[M + K]^+$, 366 (28) $[M + Na]^+$, 344 (73) $[M + H]^+$, 182 (25).

β-Xyl-Py-NHAc (6). Prepared as described above for **4**, from a solution of **(AcO)$_3$-β-Xyl-Py-NHAc 19** (96.0 mg, 0.218 mmol) in MeOH. The solution was acidified to pH = 6 with IR-120 ion-exchange resin, and the resin was removed by filtration. Evaporation of the solvent under reduced pressure and purification by column chromatography (SiO_2, EtOAc/MeOH 7:3) afforded **β-Xyl-Py-NHAc 6** (50.2 mg, 74%) as a white powder. R_f = 0.61 (EtOAc/MeOH 1:1 v/v). $[\alpha]^D_{22} = +10.77$ (c = 0.8 in DMSO). ^{1}H NMR (200 MHz, [D$_6$] DMSO): δ = 1.95 (s, 3H, CH_3), 3.00−4.00 (m, 5H, 5CH), 3.78 (s, 3H, CH_3), 4.77 (dd, J = 9.2 Hz, 8.6 Hz, 1H, CH1), 4.89 (d, J = 4.8 Hz, 1H, OH), 4.96 (d, J = 3.8 Hz, 1H, OH), 5.06 (d, J = 2.6 Hz, 1H, OH), 6.81 (s, 1H, CH), 7.14 (s, 1H, CH), 8.35 (d, J = 8.6 Hz, 1H, NH5), 9.80 (s, 1H, NH4). ^{13}C NMR (400 MHz, [D$_6$] DMSO): δ = 23.0 (CH_3), 36.2 (CH_3), 67.4 (CH_2), 69.7 (CH), 71.6 (CH), 77.7 (CH), 80.5 (CH), 104.4 (CH), 118.4 (CH), 122.0 (C), 122.2 (C), 161.3 (HNCO), 166.5 (HNCO). MS (ES+) m/z (%): 649 (59) $[2M + Na]^+$, 336 (34) $[M + Na]^+$, 314 (100) $[M + H]^+$. Elemental analysis calcd (%) for $C_{13}H_{19}O_6N_3$ (313.13): C, 49.84; H, 6.11; N, 13.41. Found: C, 49.57; H, 6.40; N, 13.21.

HO-γ-Py-Ind (7). A solution of **EtO-γ-Py-Ind 23** from the previous coupling reaction [13.6 g of a 2.54 equiv of **23** (9.76 g, 24.6 mmol) and 1 equiv of diisopropylurea] in MeOH (850 mL) were treated with aqueous NaOH (1 M, 525 mL). An instantaneous yellow color corresponded with reaction to completion, and after filtration at reduced pressure the filtrate was acidified to pH = 1 with aqueous HCl (1 M). A sticky, biscuit-colored aggregate was collected by filtration at reduced pressure and dried under vacuum at 40 °C overnight to afford the title compound as an off-white amorphous solid (7.52 g, 83%). Mp = 139−142 °C. IR (KBr): ν = 3600−2700, 1713, 1640 cm^{-1}. ^{1}H NMR (200 MHz, $CDCl_3$): δ = 1.73 (m, 2H), 2.27 (t, J = 7.1 Hz, 2H), 3.24 (m, 2H), 3.84 (s, 3H), 6.90 (d, J = 1.8 Hz, 1H), 7.05 (m, 1H), 7.23 (m, 2H), 7.31 (s, J = 1.6 Hz, 1H), 7.47 (d, J = 8.2 Hz, 1H), 7.65 (d, J = 7.9 Hz, 1H), 8.14 (t, J = 5.5 Hz, 1H), 10.38 (br s, 1H), 11.67 (br s, 1H). ^{13}C NMR (125 MHz, $CDCl_3$): δ = 24.9, 31.3, 36.1, 38.0, 103.0, 104.2, 112.4, 118.2, 119.9, 121.7, 121.8, 123.3, 123.5, 127.2, 131.8, 136.7, 158.3, 161.4, 174.5. MS (ES+) m/z (%): 759 (77) $[2M + Na]^+$, 391 (34) $[M + Na]^+$, 369 (77) $[M + H]^+$, 167 (55), 145 (100). Elemental analysis calcd (%) for $C_{19}H_{20}N_4O_4$ (368.4): C, 61.95; H, 5.47; N, 15.21. Found: C, 61.67; H, 5.31; N, 15.40.

MeNH-γ-Py-Ind (8). The activation reaction of **HO-γ-Py-Ind 7** (300 mg, 0.844 mmol) with DIPC (119 μL, 0.757 mmol) and HOBt (114 mg, 0.757 mmol) in DMF (5 mL) (room temperature, 24 h) was followed by addition of methylamine hydrochloride (102 mg, 1.51 mmol) and Et_3N (422 μL, 3.03 mmol) in DMF (5 mL) (24 h). Purification of the residue by column chromatography (SiO_2, 1−10% MeOH in CH_2Cl_2) afforded the title compound as an off-white amorphous solid (230 mg, 80%). Trituration of this solid with MeOH and then Et_2O afforded analytically pure **8** (140 mg). Mp = 240−242 °C. IR (KBr): ν = 1645, 1631, 1579, 1570 cm^{-1}. ^{1}H NMR (200 MHz, [D$_6$] DMSO): δ = 1.71 (m, 2H), 2.10 (m, 2H), 2.56 (d, J = 4.4 Hz, 3H), 3.17 (m, 2H), 3.83 (s, 3H), 6.87 (d, J = 2.0 Hz, 1H), 7.05 (dd, J = 7.4 Hz, 7.6 Hz, 1H), 7.19 (dd, J = 7.4 Hz, 7.0 Hz, 1H), 7.29 (d, J = 1.4 Hz, 2H), 7.45 (d, J = 8.0 Hz, 1H), 7.66 (m, 1H), 7.79 (m, 1H), 8.11 (dd, J = 5.8 Hz, 5.6 Hz, 1H), 10.33 (br s, 1H), 11.64 (br s, 1H). ^{13}C NMR (50 MHz, [D$_6$] DMSO): δ = 25.3, 25.4, 32.9, 35.8, 38.2, 102.8, 104.0, 112.2, 118.0, 119.7, 121.4, 121.5, 123.3, 123.3, 127.1, 131.6, 136.5, 158.2, 161.1, 172.2. MS (ES+) m/z (%): 785 (15) $[2M + Na]^+$, 763 (9) $[2M + H]^+$, 404 (5) $[M + Na]^+$, 382 (100) $[M + H]^+$. Elemental analysis calcd (%) for $C_{20}H_{23}N_5O_3$ (381.43): C, 62.98; H, 6.08; N, 18.36. Found: C, 62.89; H, 6.38; N, 18.65.

(AcO)$_4$-β-Gal-Py-NO$_2$ (9). A mixture of 1-methyl-4-nitropyrrole-2-carboxylic acid **13**[41] (108 mg, 0.634 mmol) was treated with thionyl chloride (560 μL, 7.68 mmol) and heated to reflux for 1 h. The mixture was cooled to room temperature, and an excess of reagent was removed under moderate vacuum (~80 mmHg) to afford the crude acid chloride **14**[42,43] as an off-white solid. Separately, the amine 2,3,4,6-tetra-*O*-acetyl-β-D-galactopyranosylamine **12**[54] was prepared (200 mg, 0.575 mmol) from the corresponding azide. The amine freshly prepared was immediately added to the crude acid chloride in anhydrous CH_2Cl_2 (5 mL) in the presence of Et_3N (80.0 μL, 0.575 mmol). The mixture was heated to reflux for 5 h, before cooling to room temperature overnight. Then the solvent was removed at reduced pressure. The residue was purified by column chromatography (SiO_2, 0.5% MeOH in CH_2Cl_2) to afford the title compound **9** as an off-white amorphous solid (250 mg, 87%). An analytical sample was prepared by recrystallization from ethanol. Mp = 180−182 °C. IR (KBr): ν = 1750, 1729, 1688, 1537, 1368, 1315 cm^{-1}. $[\alpha]^D_{23} = +3.29$ (c = 2.47 in acetone). ^{1}H NMR (200 MHz, [D$_6$] DMSO): δ = 1.92 (s, 6H), 1.99 (s, 3H), 2.13 (s, 3H), 3.90 (s, 3H), 4.02 (m, 2H), 4.36 (t, J = 6.1 Hz, 1H), 5.36−5.21 (m, 3H), 5.50 (t, J = 9.2 Hz, 1H), 7.58 (d, J = 2.0 Hz, 1H), 8.18 (d, J = 2.0 Hz, 1H), 9.21 (br d, J = 9.5 Hz, 1H). ^{13}C NMR (100 MHz, [D$_6$] DMSO): δ = 20.4, 20.5, 20.6 (fourth acetate signal not observed), 37.7, 61.4, 67.6, 68.2, 71.0, 71.4, 77.3, 109.1, 125.0, 128.8, 133.9, 159.9, 169.2, 169.5, 170.0, 170.0. MS (ES+) m/z (%): 1021 (4) $[2M + Na]^+$, 522 (100) $[M + Na]^+$, 500 (82) $[M + H]^+$, 331 (78) [M-(NHCO-Py-NO$_2$)]$^+$, 128 (59). Elemental analysis calcd (%) for $C_{20}H_{25}N_3O_{12}$ (499.4): C, 48.10; H, 5.05; N, 8.41. Found: C, 48.40; H, 5.35; N, 8.56.

(AcO)$_4$-β-Glc-Py-NO$_2$ (10). Prepared as for **9** described above using carboxylic acid **13** (1.00 g, 5.88 mmol) and thionyl chloride (5.15 mL, 70.6 mmol) (reflux, 3 h). A solution of a freshly prepared 2,3,4,6-tetra-*O*-acetyl-β-D-glucopyranosylamine **15**[55] (200 mg, 0.575 mmol) with Et_3N (80.0 μL, 0.575 mmol) in CH_2Cl_2 (20 mL) was added. The reaction was stirred at room temperature overnight. Purification by column chromatography (SiO_2, EtOAc) afforded the title compound **10** as an off-white amorphous solid (2.37 g, 89%). An analytical sample was prepared by recrystallization from EtOH/MeOH (20:1 v/v). Mp = 185−186 °C. IR (KBr): ν = 1750, 1530, 1314, 1232, cm^{-1}. $[\alpha]^D_{24} = -36.7$ (c = 1.64 in acetone). ^{1}H NMR (200 MHz, [D$_6$] DMSO): δ =

(54) Christiansen-Brams, I.; Meldal, M.; Bock, K. *J. Chem. Soc., Perkin Trans. 1* **1993**, 1461−1471.
(55) Takeda, T.; Sugiura, Y.; Ogihara, Y.; Shibata, S. *Can. J. Chem.* **1980**, *58*, 2600−2603.

1.92 (s, 3H), 1.95 (s, 3H), 2.00 (s, 6H), 3.91 (s, 3H), 3.96−4.23 (m, 3H), 4.92 (dd, J = 9.7, 9.9 Hz, 1H), 5.03 (dd, J = 9.3, 9.5 Hz, 1H), 5.40 (dd, J = 9.5, 9.5 Hz, 1H), 5.56 (dd, J = 9.3, 9.3 Hz, 1H), 7.53 (d, J = 1.9 Hz, 1H), 8.18 (d, J = 1.9 Hz, 1H), 9.14 (d, J = 9.3 Hz, 1H). ^{13}C NMR (50 MHz, [D_6] DMSO): δ = 20.2, 20.3, 20.5 (fourth acetate signal not observed), 37.3, 61.6, 67.8, 70.5, 72.1, 72.9, 77.0, 106.7, 124.9, 128.6, 133.8, 159.8, 168.9, 169.2, 169.4, 169.8. MS (ES+) *m*/*z* (%): 1021 (2) [2M + Na]$^+$, 522 (27) [M + Na]$^+$, 500 (100) [M + H]$^+$, 412 (27), 390 (32), 348 (55), 331 (23). Elemental analysis calcd (%) for $C_{20}H_{25}N_3O_{12}$ (499.4): C, 48.10; H, 5.05; N, 8.41. Found: C, 47.96; H, 5.22; N, 8.32.

(AcO)$_3$-*β*-Xyl-Py-NO$_2$ (11). 2,3,4-Tri-*O*-acetyl-*β*-D-xylopyranosylamine **16** obtained by hydrogenation of the correspondent azide (1.01 g, 3.35 mmol) was added to a mixture of **HO-Py-NO$_2$ 13** (525 mg, 3.09 mmol), HOBt (626 mg, 4.63 mmol), and DIPC (725 μL, 4.63 mmol) dissolved in DMF (4.0 mL) previously stirred at room temperature for 24 h. After 16 h, the residue was washed with aqueous sodium hydrogen carbonate then with water, dried over Na_2SO_4, and filtered. After solvent evaporation, the residue was purified by column chromatography (SiO_2, CH_2Cl_2/EtOAc 8:2) to afford **(AcO)$_3$-Xyl-Py-NO$_2$** (1.0 g, 70%) as a gum containing a mixture of α and β isomers (α:β = 1:5). An analytical sample of the β-isomer was separated and characterized. **(AcO)$_3$-*β*-Xyl-Py-NO$_2$ 11**: R_f = 0.39 (CH_2Cl_2/EtOAc 8:2 v/v). $[\alpha]^D_{30}$ = −53.9 (c = 1 in chloroform). ^{1}H NMR (200 MHz, $CDCl_3$): δ = 2.05 (s, 3H, CH_3), 2.10 (s, 3H, CH_3), 2.11 (s, 3H, CH_3), 3.47 (dd, J = 10.8 Hz, 11.2 Hz, 1H, CH), 3.99 (s, 3H, CH_3), 4.11 (dd, J = 5.4 Hz, 11.4 Hz, 1H, CH), 5.05 (m, 1H, CH), 5.07 (t, J = 9.4 Hz, 1H, CH), 5.22 (dd, J = 8.8 Hz, 9.2 Hz, 1H, CH1), 5.38 (dd, J = 9.6 Hz, 9.4 Hz, 1H, CH), 7.19 (d, J = 1.8 Hz, 1H, CH), 7.20 (d, J = 8.6 Hz, 1H, NH), 7.58 (d, J = 1.8 Hz, 1H, CH). ^{13}C NMR (300 MHz, $CDCl_3$): δ = 20.4 (CH_3), 20.5 (CH_3), 20.7 (CH_3), 38.1 (CH_3), 64.3 (CH5), 68.9 (CH), 71.2 (CH), 72.3 (CH), 78.5 (CH1), 108.7 (C), 124.8 (C), 127.5 (CH), 135.1 (CH), 160.4 (CONH), 169.9 ($COCH_3$), 170.1 ($COCH_3$), 171.8 ($COCH_3$). MS (ES+) *m*/*z* (%): 687 (12.5) [2M + Na]$^+$, 450 (62.5) [M + Na]$^+$, 428 (100) [M + H]$^+$. Elemental analysis calcd (%) for $C_{17}H_{21}O_{10}N_3$ (427.36): C, 47.78; H, 4.95; O, 37.44. Found: C, 47.53; H, 4.97; N, 9.66.

(AcO)$_4$-*β*-Gal-Py-NHAc (17). A solution of **(AcO)$_4$-*β*-Gal-Py-NO$_2$ 9** (400 mg, 0.801 mmol) in MeOH (20 mL) and EtOH (20 mL) was treated with 10% Pd−C (85 mg, 10 mol %) and shaken under an atmosphere of hydrogen at 45 psi overnight. The mixture was filtered, and the solvent removed under reduced pressure. The residue was taken up in CH_2Cl_2 (5 mL) and treated with a solution of acetyl chloride (63.0 μL, 0.881 mmol) and Et_3N (123 μL, 0.881 mmol) in CH_2Cl_2 (5 mL) dropwise and then stirred at room-temperature overnight. Evaporation of the solvent and purification of the residue by repeated column chromatography (SiO_2, EtOAc) afforded the title compound as a glassy film (83.0 mg, 20%). Mp = 123−125 °C. IR (KBr): ν = 1750, 1667, 1252, 1231 cm^{-1}. $[\alpha]^D_{23}$ = − 7.05 (c = 0.87 in acetone). ^{1}H NMR (200 MHz, $CDCl_3$): δ = 2.01 (s, 3H), 2.02 (s, 3H), 2.03 (s, 3H), 2.11 (s, 3H), 2.16 (s, 3H), 3.86 (s, 3H), 4.08−4.12 (m, 3H), 5.18−5.31 (m, 3H), 5.48 (br s, 1H), 6.40 (d, J = 1.6 Hz, 1H), 6.87 (d, J = 8.6 Hz, 1H), 7.29 (d, J = 1.6 Hz, 1H), 7.68 (br s, 1H). ^{13}C NMR (50 MHz, $CDCl_3$): δ = 20.5, 20.6, 20.7, 20.9, 23.6, 36.8, 61.0, 67.2, 68.4, 70.8, 72.1, 78.8, 103.9, 120.8, 121.4, 121.5, 160.8, 167.4, 169.8, 170.1, 170.4, 171.9. MS (ES+) *m*/*z* (%): 1047 (10) [2M + Na]$^+$, 1024 (14) [2M + H]$^+$, 513 (100) [M + H]$^+$. Elemental analysis calcd (%) for $C_{22}H_{29}N_3O_{11}$ + H_2O (528.5): C, 49.90; H, 5.90; N, 7.93. Found: C, 50.20; H, 5.60; N, 7.64.

(AcO)$_4$-*β*-Glc-Py-NHAc (18). Prepared as for **17** described above from **(AcO)$_4$-*β*-Glc-Py-NO$_2$ 10** (500 mg, 1.00 mmol) and 10% Pd−C (106 mg, 10 mol %) in MeOH (30 mL) (H_2, rt, 18 h). The crude material was purified by column chromatography (SiO_2, 50% EtOAc/hexane) and then precipitation from $CHCl_3$ with hexane to afford the title compound as a white amorphous solid (190 mg, 37%). Mp = 120−123 °C. IR (KBr): ν = 1751, 1655, 1233 cm^{-1}. $[\alpha]^D_{27}$ = −16.6 (c = 1.34 in [D_6] DMSO). ^{1}H NMR (300 MHz, [D_6] DMSO): δ = 1.88 (s, 3H), 1.93 (s, 3H), 1.94 (s, 3H), 1.98 (s, 6H), 3.77 (s, 3H), 3.98 (dd, J = 1.8 Hz, 12.2 Hz, 1H), 4.07−4.18 (m, 2H), 4.92 (t, J = 9.3 Hz, 1H), 5.07 (t, J = 9.0 Hz, 1H), 5.35 (t, J = 9.6 Hz, 1H), 5.50 (t, J = 9.3 Hz, 1H), 6.72 (d, J = 1.8 Hz, 1H), 7.17 (d, J = 1.8 Hz, 1H), 8.64 (d, J = 9.5 Hz, 1H), 9.79 (s, 1H). ^{13}C NMR (50 MHz, [D_6] DMSO): δ = 20.2, 20.2, 20.2, 20.4, 22.8, 35.9, 61.7, 67.9, 70.6, 72.0, 73.1, 77.1, 104.8, 118.9, 121.4, 122.1, 160.8, 166.4, 168.8, 169.1, 169.3, 169.8. MS (ES+) *m*/*z* (%): 1045 (31) [2M + Na]$^+$, 1023 (38) [2M + H]$^+$, 542 (25) [M + K]$^+$, 534 (34) [M + Na]$^+$, 512 (100) [M + H]$^+$. Elemental analysis calcd (%) for $C_{22}H_{29}N_3O_{11}$ (511.48): C, 51.66; H, 5.71; N, 8.22. Found: C, 51.38; H, 5.63; N, 8.04.

(AcO)$_3$-*β*-Xyl-Py-NHAc (19). A mixture of α and β anomers of **(AcO)$_3$-Xyl-Py-NO$_2$** (550.0 mg, 1.28 mmol) dissolved in MeOH (10 mL) and CH_2Cl_2 (5 mL) was treated with 10% Pd/C (68.5 mg, 5 mol %) and hydrogenated overnight. The mixture was filtered over a pad of Celite, and the solvent was removed under reduced pressure. The residue was taken up in CH_2Cl_2 (10 mL), and acetic anhydride (280 μL, 3.14 mmol) and Et_3N (435 μL, 3.14 mmol) were added and stirred at room temperature overnight. The mixture was evaporated under reduced pressure and purified by column chromatography (EtOAc 100%) to afford a mixture of α and β anomers (α:β = 1:5) of **(AcO)$_3$-Xyl-Py-NHAc** (394 mg, 72%). An analytical sample of each isomer was separated and characterized. **(AcO)$_3$-*β*-Xyl-Py-NHAc 19**: R_f = 0.26 (EtOAc 100%). $[\alpha]^D_{30}$ = −52.5 (c = 1 in chloroform). ^{1}H NMR (200 MHz, $CDCl_3$): δ = 2.07, 2.05 (s, 9H, 3CH_3), 2.11 (s, 3H, CH_3), 3.48 (dd, J = 11.4 Hz, 10.6 Hz, 1H, CH), 3.88 (s, 3H, CH_3), 4.09 (dd, J = 6.0 Hz, 11.5 Hz, 1H, CH), 4.95 (dd, J = 9.4 Hz, 9.6 Hz, 1H, CH), 5.02 (m, 1H, CH), 5.18 (dd, J = 9.0 Hz, 9.2 Hz, 1H, CH), 5.35 (dd, J = 9.4 Hz, 9.6 Hz, 1H, CH1), 6.32 (d, J = 1.8 Hz, 1H, CH), 6.73 (d, J = 9.0 Hz, 1H, NH5), 7.16 (s, 1H, NH4), 7.29 (d, J = 1.8 Hz, 1H, CH). ^{13}C NMR (200 MHz, $CDCl_3$): δ = 20.5 (CH_3), 20.6 (CH_3), 20.7 (CH_3), 23.4 (CH_3), 36.7 (CH_3), 64.3 (CH), 69.1 (CH), 70.9 (CH), 72.2 (CH), 79.0 (CH1), 104.3 (C), 120.9 (C), 121.5 (C), 121.6 (C), 161.3 (HNCO), 167.6 (HNCO), 169.9 ($COCH_3$), 170.0 ($COCH_3$), 171.6 ($COCH_3$). MS (ES+) *m*/*z* (%): 901 (49) [2M + Na]$^+$, 879 (33.5) [2M + H]$^+$, 462 (15.4) [M + Na]$^+$, 440 (100) [M + H]$^+$. Elemental analysis calcd (%) for $C_{19}H_{25}O_9N_3$ (439.42): C, 51.93; H, 5.73; N, 9.56. Found: C, 51.68; H, 5.69; N, 9.37. **(AcO)$_3$-α-Xyl-Py-NHAc:** R_f = 0.20 (EtOAc 100%). $[\alpha]^D_{28}$ = − 4.09 (c = 1 in chloroform). ^{1}H NMR (200 MHz, $CDCl_3$): δ = 2.11 (s, 3H, CH_3), 2.13 (s, 3H, CH_3), 2.14 (s, 3H, CH_3), 2.17 (s, 3H, CH_3), 3.88 (s, 3H, CH_3), 4.00 (m, 2H, 2CH), 4.76 (m, 1H, CH), 4.87 (dd, J = 2.7 Hz, 4.3 Hz, 1H, CH), 5.24 (t, J = 4.2 Hz, 1H, CH), 5.70 (dd, J = 8.7 Hz, 2.7 Hz, 1H, CH1), 6.52 (d, J = 2.2 Hz, 1H, CH), 6.65 (d, J = 8.8 Hz, 1H, NH5), 7.14 (d, J = 1.8 Hz, 1H, CH), 7.20 (s, 1H, NH4). ^{13}C NMR (200 MHz, $CDCl_3$): δ = 20.7 (CH_3), 20.8 (2CH_3), 23.4 (CH_3), 36.7 (CH_3), 63.8 (CH_2), 66.7 (CH), 67.5 (CH), 68.6 (CH), 74.5 (CH), 104.6 (C), 120.3 (C), 121.5 (C), 121.8 (C), 161.1 (HNCO), 167.7 (HNCO), 169.1 ($COCH_3$), 169.6 ($COCH_3$), 169.8 ($COCH_3$). MS (ES+) *m*/*z* (%): 879 (3) [2M + H]$^+$, 462 (100) [M + Na]$^+$, 440 (65) [M + H]$^+$. Elemental analysis calcd (%) for $C_{19}H_{25}O_9N_3$ (439.42): C, 51.93; H, 5.73; N, 9.56. Found: C, 51.58; H, 6.02; N, 9.18.

EtO-*γ*-Py-NO$_2$ (20). The title compound was prepared according to the method of Xiao et al.[44] with 1-methyl-4-nitro-2-trichloroacetylpyrrole (1.00 g, 3.91 mmol), Et_3N (1.20 mL, 8.62 mmol), ethyl-4-aminobutyrate hydrochloride (721 mg, 4.31 mmol), and EtOAc (20 mL) to afford the target ester after 24 h at room temperature. Then, it was purified by column chromatography (SiO_2, EtOAc) as yellow oil (1.00 g, 90%) which slowly crystallized on standing. An analytical sample was prepared by precipitation from ethanol at room temperature overnight to afford an off-white amorphous solid. Mp = 68−70 °C; R_f = 0.53 (AcOEt/hexane 6:4 v/v). IR (KBr):[44] ν = 1728, 1666, 1526, 1318 cm^{-1}. ^{1}H NMR (200 MHz, $CDCl_3$): δ = 1.26 (t, J = 7.2 Hz, 3H), 1.94 (t, J = 6.6 Hz, 2H), 2.44 (t, J = 6.6 Hz, 2H), 3.43 (q, J = 6.6 Hz, 2H), 3.98 (s, 3H), 4.16 (q, J = 7.2 Hz, 2H), 6.59 (br s, 1H),

7.09 (d, J = 1.8 Hz, 1H), 7.55 (d, J = 1.8 Hz, 1H). ^{13}C NMR (200 MHz, $CDCl_3$): δ = 14.0 (CH_3), 24.2 (CH_2), 31.8 (CH_2), 37.8 (CH_3), 39.1 (CH_2), 60.7 (CH_2), 106.9 (CH), 126.4 (C), 126.6 (CH), 134.7 (C), 160.4 (CO), 173.7 (CO). MS (ES+) m/z (%): 589 (8) $[2M + Na]^+$, 306 (45) $[M + Na]^+$, 284 (100) $[M + H]^+$. Elemental analysis calcd (%) for $C_{12}H_{17}N_3O_5$ (283.28): C, 50.88; H, 6.05; N, 14.83. Found: C, 51.02; H, 6.05; N, 15.10.

EtO-γ-Py-Ind (23). A mixture of **EtO-γ-Py-NO$_2$ 20** (10.0 g, 35.3 mmol) and 10% Pd−C (1.87 g, 5 mol %) was stirred in ethyl acetate (200 mL) under an atmosphere of hydrogen at 45 psi for 24 h. The catalyst was removed by filtration under gravity and the solvent removed under reduced pressure to afford 9.90 g of brown oil. To a solution of this oil in anhydrous CH_2Cl_2 (150 mL) was added 2-indole carboxylic acid **22** (6.83 g, 42.4 mmol), DMAP (5.18 g, 42.4 mmol), HOBt (5.72 g, 42.4 mmol), and DIPC (6.63 mL, 42.4 mmol) and stirring under an argon atmosphere at room temperature overnight. The solvent was removed under reduced pressure, and the residue purified by column chromatography (SiO_2, 50% EtOAc in hexane) to afford the title compound **23** with a percentage of diisopropylurea (13.6 g, **23**/urea (2.54:1) by ^{1}H NMR by wt. 9.76 g, 70% yield of **23**). The crude material was used immediately for preparation of the acid **7** (see below). To characterize a pure sample of the ester **23**, the following reaction was performed. A slurry of **HO-γ-Py-Ind 7** (0.250 g, 0.679 mmol) in absolute EtOH (10 mL) was treated with concentrated H_2SO_4 (3 drops) and heated to reflux. Slow dissolution of the carboxylic acid substrate was indicative of complete conversion (after 2 h), confirmed by TLC analysis (EtOAc). The solvent was removed under reduced pressure, and the residue was purified by column chromatography (SiO_2, EtOAc) to afford the title compound as crispy white foam (270 mg, 99%). An analytical sample was prepared by trituration with EtOAc then Et_2O to give **23** as white waxy flakes (190 mg). Mp = 165−166 °C; R_f = 0.596 (AcOEt 100%). IR (KBr): ν = 1717, 1653, 1640 cm^{-1}. ^{1}H NMR (200 MHz, DMSO): δ = 1.18 (t, J = 7.0 Hz, 3H), 1.75 (m, 2H), 2.33 (t, J = 7.4 Hz, 2H), 3.21 (q, J = 6.0 Hz, 2H), 3.83 (s, 3H), 4.05 (q, J = 7.0 Hz, 2H), 6.88 (d, J = 1.8 Hz, 1H), 7.05 (t, J = 7.5 Hz, 1H), 7.19 (t, J = 8.0 Hz), 7.29 (m, 2H), 7.46 (d, J = 7.8 Hz, 1H), 7.65 (d, J = 7.8 Hz, 1H), 8.11 (t, J = 5.8 Hz, 1H), 10.31 (s, 1H), 11.31 (s, 1H). ^{13}C NMR (125 MHz, [D_6] DMSO): δ = 14.1 (CH_3), 24.8 (CH_2), 31.1 (CH_2), 36.1 (CH_3), 37.8 (CH_2), 59.8 (CH_2), 102.8 (CH), 104.1 (CH), 112.3 (CH), 118.2 (CH), 119.8 (CH), 121.6 (CH), 121.7 (C), 123.2 (C), 123.4 (CH), 127.2 (C), 131.7 (C), 136.6 (C), 158.3 (CO), 161.3 (CO), 172.8 (CO). MS (ES+) m/z (%): 816 (13) $[2M + Na]^+$, 419 (4) $[M + Na]^+$, 397 (100) $[M + H]^+$. Elemental analysis calcd (%) for $C_{21}H_{24}N_4O_4$ (396.4): C, 63.62; H, 6.10; N, 14.13. Found: C, 63.50; H, 6.10; N, 14.00.

Structural Studies. ^{1}H NMR Experiments. All the spectra in aqueous solution were recorded with presaturation of the water signal. The chemical shifts were reported in ppm relative to DSS (0.00 ppm) when D_2O was used and relative to residual acetone (2.04 ppm) when D_2O/[D_6]-acetone or H_2O/[D_6]-acetone was used in the experiment. NMR structural studies of compounds **1**−**8** were based on monodimensional and bidimensional (COSY, TOCSY, NOESY, ROESY) spectra and were recorded at 300, 400, or 500 MHz and 26 °C in a Varian instrument. Sample solutions were prepared at concentrations ranging between 5 and 0.1 mM, depending on the solubility of the compounds. The spectra for compound **7** were recorded at 0.1 mM in D_2O, where no self-association occurs.

Dilution Experiments. Dilution experiments of compounds **1**−**8** were carried out in D_2O/[D_6]-acetone, in H_2O/D_2O, and in D_2O, at 26 °C. Concentrations of the sugar−oligoamides ranged between 10 mM and 0.1 mM in D_2O/[D_6]-acetone. A dilution experiment in D_2O started with a saturated NMR sample of the sugar−oligoamide, due to its poor solubility in water, and was diluted, until a concentration of 0.1 mM was reached. Only compound **7** showed significant chemically induced shift of the proton resonances upon dilution of the sample in D_2O. K_a = 100 M^{-1} was found for the autoassociation process of **7** (assuming association to dimer only). Compounds **1**−**6** and **9** do not autoassociate under the experimental conditions used.

Molecular Modeling. Molecular models for **β-Xyl-Py-γ-Py-Ind** and **α-Xyl-Py-γ-Py-Ind** were generated employing the MM2* force field as implemented in Macromodel 5.5. As a first step, a constrained minimization was performed including the NOE derived distances as experimental constrains. The obtained geometries were then subjected to unconstrained minimizations, using 5000 conjugate gradients iterations, and the GB/SA solvent model for the treatment of water.

DNA Interaction with *ct*-DNA of 1−3, 6, 7, and Netropsin. All NMR interaction experiments have been carried out in phosphate buffer (10 mM, pH = 7). The binding abilities of the different ligands to calf thymus DNA (*ct*-DNA) were investigated from ^{1}H NMR titration experiments. Ligand samples were prepared at a constant concentration of 0.1 mM. The *ct*-DNA titrant sample (stock solution) was prepared by dissolving 2 mg of *ct*-DNA into 0.7 mL solution of 0.1 mM in ligand. The concentration of *ct*-ADN was calculated by UV/vis spectroscopy (c = 3.58 × 10^{-3} M), using ϵ_{260} = 6600 M^{-1} cm^{-1}.[56] Then, 0.6 mL of the ligand solution was introduced into the NMR tube, and increasing amounts of the titrant DNA solution were added. A 1D-NMR spectrum was recorded in the same "acquisition mode" (nt = 256, Temp = 26 °C) after each addition of *ct*-DNA. A progressive broadening and disappearance of the proton signals from the ligand was observed indicating the binding of the ligand to *ct*-DNA.

Blank Experiments. (1) A 0.1 mM solution in *O*-methyl-α-D-glucopyranoside and 0.1 mM in sugar−oligoamide was used to prepare a stock solution of *ct*-DNA under the same conditions as described above. Then, a titration experiment was carried out. *O*-Methyl-α-D-glucopyranoside resonances that appear between 3 and 4 ppm did not experience any change in intensity or line widths, while oligoamide resonances progressively disappeared upon addition of *ct*-DNA. (2) A blank experiment was also carried out, titrating a 0.1 mM solution of *O*-methyl-α-D-glucopyranoside with a stock solution of *ct*-DNA in the same conditions. No changes in the glucopyranoside spectrum were observed after addition of large amounts of DNA indicating that no binding takes place.

Interaction Studies with poly(dA-dT) and poly(dG-dC). The binding abilities of sugar−oligoamides **1** and **3** to poly(dA-dT) and poly(dG-dC) were investigated by ^{1}H NMR titration experiments. Ligand samples were prepared at a constant concentration of 0.1 mM. Poly(dA-dT) and poly(dG-dC) titrant samples (stock solution) were prepared dissolving, in the case of poly (dA-dT), 50 unities of the oligonucleotide in 2 mL of a solution 10^{-4} M of the ligand. Under these conditions, the concentration of poly(dA-dT) was 3.79 mM bp (ϵ_{258} = 13 200 M^{-1} cm^{-1}).[57] In the case of the Netropsin titration, the concentration of poly(dA-dT) was 3.79 × 10^{-2} mM bp.

The concentration of poly (dG-dC) was 2.12 mM bp (ϵ_{256} = 16 800 M^{-1} cm^{-1})[57] for all titrations, obtained by dissolving 25 unities of the oligonucleotide in 0.5 mL of a 10^{-4} M solution of the ligand. Titrations were carried out as described for *ct*-DNA.

Competition Experiment of 3 with Netropsin. Competition experiments for **3** were carried out in D_2O (phosphate buffer 10 mM, pH = 7) by ^{1}H NMR titration in the Varian Inova-300 equipment. The temperature was 26 °C. The free ligand sample was a saturated solution of glyco-oligoamide in D_2O, prepared by dissolving 1.5 mg of the ligand in 1 mL. The concentration of the solution was 3 × 10^{-4} M. Then, increasing amounts of a solution of *ct*-DNA 3.6 × 10^{-2} M were added to the NMR tube until the complete disappearance of the resonances of **3** in the ^{1}H NMR spectra was achieved. Then, increasing amounts of one solution of Netropsin (10^{-2} M) were added.

TR-NOESY Experiments. TR-NOESY experiments for the bound ligand were recorded on a 300 MHz spectrometer (Bruker) and 500

(56) Barton, J. K.; Goldberg, J. M.; Kumar, C. V.; Turro, N. J. *J. Am. Chem. Soc.* **1986**, *108*, 2081.
(57) Lootiens, F. G.; Regenfuss, P.; Zechel, A.; Lieve, D.; Clegg, R. M. *Biochemistry* **1990**, *29*, 9029−9039.

MHz spectrometers (Varian and Bruker) with saturation of the residual H_2O signal or with the Watergate pulse sequence. Sugar oligoamide solutions were prepared at saturation (1 mg/0.6 mL D_2O), but the operating concentration was 0.5 mM, after sonication of the NMR sample. Further addition of the *ct*-DNA solution (2 mg/0.7 mL D_2O or H_2O with 15% D_2O) to the NMR sample induced broadening in the resonance signals of the sugar−oligoamide. This fact is a clear indication of binding of the ligand to *ct*-DNA.

TR-NOESY experiments were recorded at 26 °C and performed with mixing times of 200, 300, and 400 ms. The experiment in H_2O/D_2O (15%) has been recorded at 18 °C.

Acknowledgment. Financial support for this work was provided by the DGES (Grant BQU2000-1501-C01, BQU2003-03550-C03-01 and -02), a European TMR project (FMRX-CT98-0231), and RTN European project (HPRN-CT-2002-00190). J.M. and C.S. thank the TMR project, and F.S. thanks the RTN project for a postdoctoral fellowship. E.M. is grateful to the Comunidad Autonoma de Madrid for a fellowship.

Supporting Information Available: Supporting Information shows relevant NMR data of the free ligand, including inter- and intrastrand NOEs, tables with chemical shifts, and details on molecular modeling. Additionally, NMR titration of ligands with *ct*-DNA and characterization of the bound state conformation by TR-NOESY experiments. This material is available free of charge via the Internet at http://pubs.acs.org.

JA050794N